Material science from the implant industry point of view

A Spiegel¹, H Polzhofer¹, M Ammann¹

Medartis AG, Basel, CH

Implants may be used for different purposes and hence the requirements placed on them vary widely. It follows that the industry producing these implants is rather heterogeneous. Rather than bundling all implants as one, different applications and classes of implants must be distinguished. A fundamental differentiator is the intended period of implantation. Implants that are to permanently replace a biological structure such as joint replacements, dental implants, or mammal implants must be biostable and remain localized in the human body. Stable integration into hard or soft tissue is typically a requirement independent of the mechanical demands which may vary widely. Hip or knee implants are subjected to high mechanical loading and difficult tribological conditions, dental implants must be abrasion resistant and meet stringent cosmetic criteria, and mammal implants should provide satisfactory tactile properties, integrate with soft tissue while preventing capsule formation.

In the following article, we will focus on plates and screws for craniomaxillofacial and trauma applications intended for bony fixation after an accidental fracture or a planned intervention. These have to meet a wide range of often contradicting requirements (shown in Table 1).

Table 1. Requirements of bone-plates and -screws

	High	Low
Mechanical	Secure fracture	Can be adapted
Strength	fixation	during surgery
Elasticity, E	Prevent micro-	No cut-through
	motion	in bad bone
Tissue	No liquid filled	Free gliding of
integration	fibrous capsules	tendons

Whereas the mechanical requirements can usually be met through an appropriate design, the correct tissue response has proven to be more difficult to provide. Especially, as there is still no general consensus as to what actually constitutes the desired response.

Traditionally, good tissue integration has been desirable even for non-permanent implants. Formation of a fibrous capsule around an implant [1] is not desirable as this may lead to the

formation of a liquid-filled immunoincompetent zone prone to pathogen proliferation [2]. Whether this is actually the case, especially in cases of large tendon displacements e.g. for finger implants is still under debate [3].

In recent years, the factors governing interaction between tissue and metal implants have been studied extensively. The questions as to whether material or topography play the main part in this interaction seems to be mostly answered in favour of topography. Summarized very briefly, the smoother a surface the less tissue integration will occur [4]. However, topography is not independent of the material chosen. And while technology to produce smooth stainless implants is cheap and readily available in the form of electropolishing the same is not true for other materials such as commercially pure Ti (cp Ti) or its alloys.



Fig. 1: Images of hand implants with 'standard' microrough surface (left) and highly polished surface (right).

Medartis has investigated methods for producing smoother cpTi implants for specific applications (e.g. hand) and has gone from simple mass finish processes followed by pickling and anodization to more sophisticated processes thereby reducing surface roughness by a factor of 2. Whether this will actually result in better clinical results still remains to be seen.

REFERENCES: ¹ J.A. Parker, X.F. Walboomers. J.W. Von den Hoff et al (2002) *Biomaterials* **23**: 3887-96 ² A.G. Gristina (1994) *Clin Orthop Relat Res* **298**:106-18. ³ J.S. Hayes and R.G. Richards (2010) *Expert Rev Med Devices* **7**:131-42. ⁴ B.D. Boyan and Z. Schwartz (1999) Modulation of osteogenesis via implant surface design in *Bone Engineering* (ed J.E. Davies) EM Squared Inc., pp 232-9.



Translating science into technology in biomaterials science: Strontium functionalized implants

M. Foss¹

¹ <u>Interdisciplinary Nanoscience Centre – iNANO</u>, Science and Technology, Aarhus University, Denmark. Email: foss@inano.au.dk

It is a challenging task to combine University research and education with more specific user-driven goals, e.g. development of novel knowledge based products and processes. With starting point in a specific successful project concerning strontium functionalization of orthopedic implants [1], I will address a few of the special challenges of pushing research results towards commercial utilization and thereby contributing to the development of business and society.

Strontium (Sr) is an alkali earth metal, which is known to be incorporated into the mineral phase of bone. It has been shown that Sr influences bone homeostasis both by inhibiting bone resorption and by increasing bone formation. Sr containing complexes has been used for the treatment of bone loss associated with e.g. osteoporosis. We developed a novel surface modification method aimed at creating a thin coating tailored for a sustained release of strontium. The coatings were prepared by a Physical Vapor Deposition (PVD) magnetron co-sputtering process and selected on the basis of Sr-release data in PBS buffer quantified by inductively coupled plasma optical emission spectroscopy (ICP-OES). A rodent study (Wistar rats) showed a significant increase in direct bone-to-implant contact and peri-implant bone volume four weeks after implantation for several of the Sr modified implant groups as compared to commercially pure grade 4 titanium, which served as reference.

This example will demonstrate that is it possible for PhD students to combine peer-reviewed articles and patents during the studies and a career in the industry.

REFERENCES: ¹ O. Z. Andersen et al. (2013) Accelerated bone ingrowth by local delivery of strontium from surface functionalized titanium Implants, *Biomaterials* **34**: 5883-5890.



Prevalence of metal sensitization in a dermatologic patient collective and in patients with symptomatic metal implants

K. Scherer Hofmeier, A.J. Bircher

Allergy Unit, Department of Dermatology, University Hospital Basel, CH.

INTRODUCTION: Patients with implanted metal devices may experience a variety of adverse reactions. Complaints include pain, swelling, inflammation, wound healing complications, and more rarely eczema. Possible causes are, apart from technical and mechanical problems, infections mainly by bacteria, toxicity to the polyethylene, foreign materials. e.g. granulomatous foreign body reactions, and possibly hyper-sensitivity reactions to alloy resulting in the above-mentioned symptoms or even loosening of the implant. Contact sensitization to Ni, Co and Cr is frequent in the general population. Due to the increasing use of metallic alloys other potential metal contact allergens are of interest. There is little information on the prevalence of sensitization in the general population and in affected patients. In this study the prevalence of contact sensitization to 14 metal salts was prospectively investigated by patch tests in 1051 dermatologic patients and in 141 patients with symptomatic metal implants.

METHODS: 15 Swiss dermatology centres participated in the first study. 1051 patients undergoing routine patch testing, incl. Ni, Co, Cr, Pd salts and thiomersal, were additionally tested with ten metals. Tests were read at 48 and 72 h. In a separate study 164 symptomatic patients were tested in Basel only, i.e. 18 hip prosthesis HTP, 100 knee prosthesis KTP, 20 with ostheosynthesis material OS, 3 shoulder prosthesis STP, 23 preoperative patients (pre-op) without any implants as controls, with up to 47 metals and bone cement components.

RESULTS: Sensitization rates to most metals were lower in patients with implants than in patients without. Surprisingly, high sensitization rates were found in symptomatic patients for PdCl, Pd, Mn, rhodium chloride (Rh). This does not imply relevance of the sensitization. Some metals tend to evoke atypical pustular test reactions (Mn, Rh) of unknown significance. Bone cement components were found to be test positive in eight KTP, two HTP and one OS and STP, each, benzoylperoxide being the most important

component. Analysis of probable relevance of patch test results is shown in the tables.

Table 1. Number of subjects tested with each allergen and the respective outcome

unergen and the respective outcome						
Metal	Negative	Positive	Positive	Positive		
	test	irritant	questionable	allergic		
	n	n	n	n		
Ni	841	8	12	182		
Pd	789	37	52	171		
Mn	697	78	140	151		
Au	914	27	25	83		
Cu	912	36	44	58		
PdCl	816	0	20	47		
Co	977	12	6	49		
Hg	974	27	14	35		
Nb	977	29	18	25		
Thio	867	0	6	19		
Cr	966	51	9	17		
Al	1007	11	16	6		
Pt	1025	14	7	4		
Mo	1028	12	7	3		
Ti	1027	16	5	2		

Table 2. Patients of part 2 sensitized to any metal with regard to type of implant (p-Value 0.0682 Fisher's exact test only for HTP and KTP).

Tisher's exact test only for 1111 and K11).						
	All	Pre-	HT	KT	OS	ST
	sample	op	P	P		P
No	75	11	11	40	11	2
pos						
Any	87	11	6	60	9	1
pos						

Conclusion: Testing of rare allergenic metals in routine patch test patients reveals, as expected, nickel to be the most common contact allergen, followed by palladium with sodium tetrachloropalladate being the more sensitive test compound. Some metals with particular pustular test reactions need further investigations.

ACKNOWLEDGEMENTS: This study was funded in part by the International Bone Research Association, research grant 0901-0079.



From engineering grafts to engineering developmental processes for regenerative medicine

I Martin¹

¹ Department of Biomedicine & Department of Surgery, <u>University</u> Hospital Basel, Basel, CH.

SUMMARY: Following the exemplifying context of cartilage and bone regeneration, this lecture will describe and discuss alternative approaches currently pursued by the author's team to evolve classical tissue engineering paradigms towards possibly more effective grafts, with the potential for a broader clinical use.

The presentation will start from a short description of the clinical trials carried out at the University Hospital Basel for alar lobule reconstruction (1) or repair of articular cartilage defects based on the engineering of autologous cell-based cartilage grafts.

The lecture will then propose and discuss the concept of engineering regenerative strategies by recapitulating developmental processes, exploiting the own body as the in vivo bioreactor (2,3).

The implementation of such paradigm will be presented in two different scenarios. The first relies on the engineering of a living, autologous cell-based hypertrophic cartilage tissue, which is capable to undergo efficient remodelling into bone tissue upon in vivo implantation, according to the biological pathway of endochondral ossification (Figure 1). The second is based on the engineering of a cellular graft, which is however decellularized and stored off-the shelf (4). The resulting material would include in the extracellular matrix the diverse, cell-produced signals required to induce bone regeneration, and may be generated using standardized cell lines as opposed to autologous cells. These cell lines could be customized by genetic engineering techniques to overexpress specific factors aimed at enhancing the potency of the graft for defined indications (e.g., to increase the efficiency of remodelling or vascularization) (5).

The perspective will also address issues related to scalability, process control and regulatory compliance in manufacturing cell-based products and highlight the need not only to automate, but also to streamline and simplify typical production processes (6).

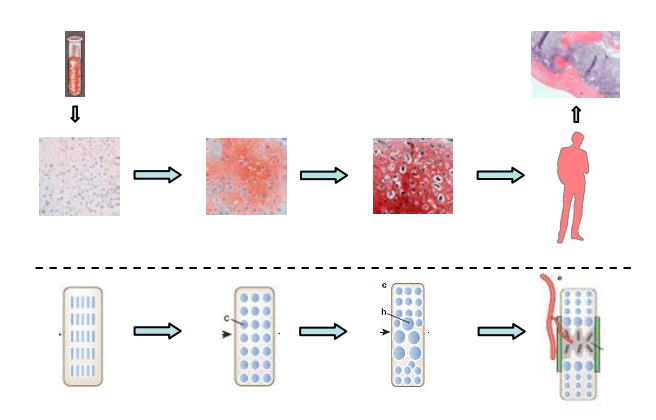


Figure 1: A "Developmental engineering" paradigm to induce tissue regeneration. Rather than engineering a tissue, the strategy targets the use of cells to engineer the different stages of a process (top part) which recapitulate events of development (e.g., endochondral ossification; bottom part). The product will be a tissue containing all necessary and sufficient cues to remodel into the target repair tissue upon grafting.

REFERENCES:

- (1) I Fulco, S Miot et al. Engineered autologous cartilage for nasal reconstruction after tumour resection: an observational first-in-human trial. *The Lancet* (2014)
- (2) C Scotti, B Tonnarelli et al. Recapitulation of endochondral bone formation using human adult mesenchymal stem cells as a paradigm for developmental engineering. *Proc. Natl Acad Sci USA* (2010)
- (3) C Scotti, E Piccinini, H Takizawa et al. Engineering of a functional bone organ through endocondral ossification. *Proc. Natl Acad Sci USA* (2013)
- (4) P Bourgine, B Pippenger at al. Tissue decellularization by activation of programmed cell death. *Biomaterials* (2013)
- (5) I Martin. Engineered tissues as customized organ germs. *Tissue Eng-A* (2014)
- (6) I Martin et al. Manufacturing challenges in regenerative medicine. Sci Transl Med (2014)

ACKNOWLEDGEMENTS: The presented work was funded by the SNF (Div III Grant No. 310030_133110/1 and Sinergia Grant No. CRSII3_136179 / 1)



Immune complement activation by a faceted nano-container in the pig model

S Bugna^{1,2}, A Weinberger³, R Urbanics⁴, B Müller¹, A Zumbuehl³, J Szebeni⁴, and T Saxer²

¹ <u>Biomaterials Science Center</u>, Universitätspital, Basel, CH. ² <u>Cardiology Division, University</u>

<u>Hospital of Geneva, Geneva, CH.</u> ³ <u>Department of Chemistry, University of Fribourg, Fribourg,</u>
CH. ⁴ <u>Nanomedicine Research and Education Center, Semmelweis University, and Seroscience Ltd,</u>

Budapest, HU

INTRODUCTION: Pharmacotherapy uses a wide range of liposomes as nano-carriers for targeted delivery or controlled release of drugs and The nano-carriers diagnostic agents. substantially alter the absorption, distribution, metabolism, and excretion of the encapsulated drugs, improving their efficacy and reducing their toxicity. However, besides their unique therapeutic advantages, these carriers share the potential problem of being recognized by the immune system as foreign, which leads to the rise of adverse reactions, loss of efficacy, and risk of anaphylactic shock. The activation of the complement (C) can result in a hypersensitivity reaction, termed C activation-related pseudoallergy (CARPA). This phenomenon frequently occurs with liposomes or lipid-based drugs and creates adverse effects, in a high percentage of people, leading occasionally to an anaphylactic reaction or even to death.

The goal of the present study was to explore the complement activation induced by artificial, facetted Pad-PC-Pad vesicles² both *in vitro* (human serum) and *in vivo*.

METHODS: The *in vivo* study comprised the injection of bolus of 0.5 and 5.0 mg lipid in three pigs. The physiological reaction, i.e. systemic arterial pressure, pulmonary arterial pressure, and heart rate, was monitored during six hours. Blood cells, thromboxane and blood biomarkers were screened for potential toxicity before and six hours after injection. The positive control was induced injecting 0.1 mg/kg of Zymosan A (Sigma-Aldrich Co. LLC.).

RESULTS: The highest physiological reaction we detected was a 30 % elevation (5 mmHg) of the pulmonary arterial pressure with 5 mg/kg of lipids of aggregated liposomes, which represents insignificant changes only. The formulation led to time-dependent liposomal aggregates that could be disrupted through filtration. We registered a decrease of lymphocytes by 20 % to 40 % in all pigs without other changes in blood cells or thromboxane. When the liposomes were filtered prior to the injection no reaction of the

complement was found. Only minor changes in the biomarkers were observed, such as the single detection of a 300 % increase of bilirubin and the concomitant increase of 200 % urea.

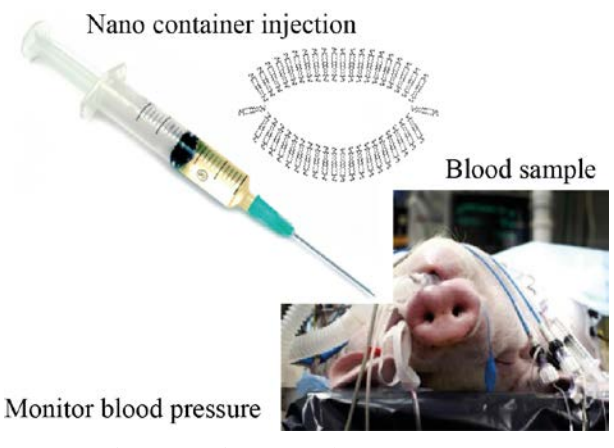


Fig. 1 Scheme of the animal experiment.

DISCUSSION & CONCLUSIONS: The present study indicates that Pad-PC-Pad liposomes extruded to 100 nm in diameter are not inducing a significant CARPA reaction (CAS 1) neither with a dose of 5 mg/kg phospholipids nor with the injection of 110 mg lipids. This result has to be related to published data that show high CARPA reactivity with pharmacologically approved liposomal formulations at a dosage between 0.01 and 0.5 mg/kg phospholipids.³ The lymphocyte decrease starts after 90 minutes only, which needs to be explored in detail. Such a long period of examination is not yet found in literature. In conclusion, Pad-PC-Pad liposomes are promising nano-containers for drug delivery.4

REFERENCES: ¹ J. Szebeni et al. (1998) *Crit Rev Ther Drug Carrier Syst.* **15**:57-88. ² M.N. Holmes (2012) *Nature Nanotechnol* **7**:536–43. ³ J. Szebeni et al. (2012) *Nanomed* **8**:176-84. ⁴ T. Saxer, A. Zumbuehl, B. Müller (2013) *Cardiovasc Res* **99**:328-33.

ACKNOWLEDGEMENTS: This work is financially supported by the Swiss National Science Foundation (NRP 62 "Smart Materials", Project NO-Stress).



Protein and blood-interaction studies on nano-roughness gradients

Rebecca P. Huber^{1,2}, Katharina Maniura-Weber², Nicholas D. Spencer¹

¹Laboratory for Surface Science and Technology, Department of Materials, ETH Zurich, CH

²Laboratory for Materials-Biology Interactions, Empa, St. Gallen, CH, rebecca.huber@mat.ethz.ch

INTRODUCTION: To investigate the influence of a surface parameter on a given process, working with individual samples requires many repetitions with the challenge of maintaining the experimental conditions constant. This approach is laborious and cost-ineffective. Roughness gradients are a very promising tool to investigate the effect of surface topography on a biological system, as a wide range of parameters can be explored in a single experiment. ^{5,6}.

The success of a surgical implant is dependent on an appropriate biological response to the implant surface¹. Wound healing around implants is a complex process in which water molecules from the surrounding blood first come in contact with the surface. In the next step, ions and blood proteins adsorb and a fibrin network is formed, before osteoblastic cells respond to the protein-covered surface².

Blood protein adsorption and blood coagulation are greatly influenced by the topography of titanium surfaces^{3,4}, which may further impact the eventual adhesion, migration and differentiation of primary human osteogenic cells on a titanium implant. It is therefore of major importance for implantology to understand the early interaction between blood and the implant and how this further steers osseointegration.

METHODS: To study the effect of nanoroughness on protein adsorption and blood coagulation, nanoparticle density gradients were fabricated (see Fig. 1a)). A flat silicon wafer was first rendered positively charged with a coating of poly(ethylene imine), and then slowly immersed into a highly diluted silica-particle suspension, to generate a linear particle-density gradient on the surface. The gradient was subsequently heattreated at 1050 °C to sinter the particles to the surface. In order to mimic the surface of implants, the samples were sputter coated with titanium. Finally, gradients were exposed the fluorescently labelled albumin, fibrinogen or fibronectin. To achieve an easy and rapid data read-out, a fluorescence micro-array scanner was used to map all adsorbed proteins.

In a second step, the same gradients were used to study blood coagulation by incubation of the gradients for 2 to 10 min with partially heparinized (0.5 IU/ml) whole human blood from healthy volunteers. The formation of the blood clot was

investigated by scanning electron microscopy and fluorescence microscopy.

RESULTS: Particles of different sizes were tested, with diameters of 12, 39 and 72 nm. The protein-adsorption experiments showed no significant influence of nano-features on protein adsorption for all sizes of nanoparticle investigated.

In Figure 1 b) SEM images along a 39 nm nanoparticle density gradient following a 5 min blood-incubation experiment are presented. It is clearly visible that the appearance of the blood clot changes along the particle-density gradient. While coagulation was observed everywhere on the sample, a denser fibrin network could be detected towards the high-density end of the gradient. Such a fibrin network is of importance for further healing of the wound, as well as for cell adhesion and differentiation.

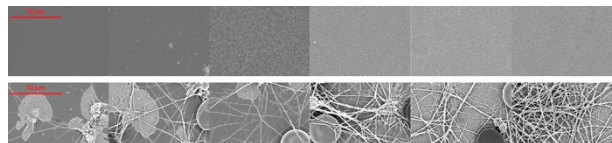


Fig. 1: SEM images taken every mm along the 39 nm nanoparticle density gradient. a) Gradient before blood incubation. b) Gradient after incubation for 5 min in whole human blood.

DISCUSSION & CONCLUSIONS: Nanostructures were shown to enhance blood

Nanostructures were shown to enhance blood coagulation, but appear to have no significant influence on protein adsorption from solutions.

This study suggests that implant surfaces with a high-density nanostructure show improved blood clot formation and should therefore enhance osseointegration

REFERENCES: ¹ C.J. Wilson et al., Tissue engineering 11, Nr. ½ (2005): 1-18 ² B. Kasemo, Surface Science 500 (2002): 656-677 ³ M.S. Lord et al, Nano Today 5, Nr.1 (2010): 66-78 ⁴ Hong J et al, Biomaterials 20 (1999): 603-11. ⁵ S. Morgenthaler et al., Soft Matter 4 (2008): 419-434. ⁶ C. Zink et al, Biomaterials 33 (2012): 8055-8061

ACKNOWLEDGEMENTS: We would like to thank ScopeM for their skillful SEM support The Swiss National Science Foundation (SNF, Grant no: CR31I3_146468) is gratefully acknowledged for funding.



"Nonswellable" hydrogel without mechanical hysteresis

H Kamata¹, U Chung^{1, 2, 3}, T Sakai¹

¹ Department of Bioengineering, School of Engineering, University of Tokyo, Japan. ² Center for Disease Biology and Integrative Medicine, Division of Clinical Biotechnology, School of Medicine, Japan. ³ Division of Tissue Engineering, University of Tokyo Hospital, Japan.

INTRODUCTION: Hydrogels are promising scaffolding materials in tissue engineering applications. However, conventional hydrogels "swell" under physiological conditions, drastically weakening their mechanical properties [1]. Herein, we report a new class of hydrogels with precisely controlled swelling behaviour.

METHODS: Hydrogels with thermoresponsive segments were prepared by mixing aqueous of tetra-armed hydrophilic thermoresponsive polymers that were synthesised via an anionic ring-opening polymerization (water content ~ 95%) (Fig. 1). The hydrogels were immersed in Dulbecco's Phosphate Buffered Saline (D-PBS), and then their equilibrium swelling ratio (Q) was measured at each temperature. Elongation and compression tests were performed using the samples equilibrated under physiological conditions (i.e., in D-PBS at 37°C).

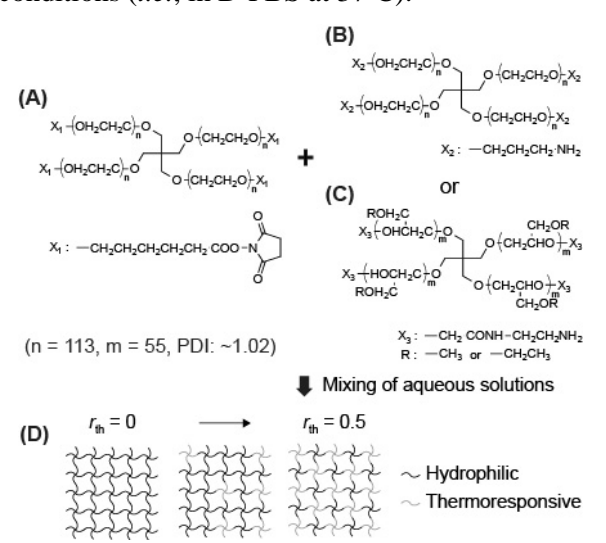


Fig. 1. Schematic of the thermoresponsive hydrogel system. (A) Hydrophilic tetra-armed poly(ethylene oxide) with active ester end-groups. (B) Hydrophilic tetra-armed poly(ethylene oxide) with amino end-groups. (C) Thermoresponsive tetra-armed poly(ethyl glycidyl ether-co-methyl glycidyl ether) with amino end-groups. (D) Polymer networks composed of hydrophilic (black) and thermoresponsive (gray) polymer units where r_{th} represents the thermoresponsive segment ratio.

RESULTS & DISCUSSION: The Q values under physiological conditions depended on r_{th} , while the hydrogel with $r_{th} = 0.4$ maintained its initial shape $(Q \sim 100\% = \text{``nonswellable''} \text{ hydrogel)}$ (Fig. 2).

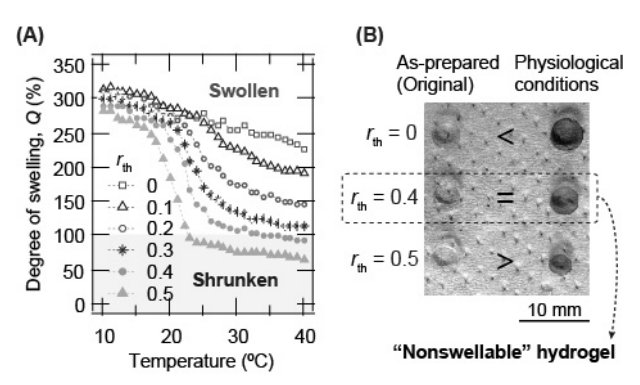


Fig. 2. Swelling behaviour of hydrogels in D-PBS. r_{th} represents the thermoresponsive segment ratio. (A) The swelling ratio (Q) as a function of temperature. $Q = V/V_0 \times 100$, where V is the volume of the samples in the equilibrium-swollen state at each temperature, and V_0 is the initial volume of the samples (i.e., before swelling). (B) Photos of the samples that exhibit different swelling degrees depending on r_{th} .

The hydrogel composed only of hydrophilic polymers ($r_{\rm th}=0$, conventional hydrogels) endured 7-fold elongation in the as-prepared state. However, the swollen hydrogel failed at 2-fold elongation. In stark contrast, "nonswellable" hydrogel endured 7-fold elongation even in its equilibrium state under physiological conditions. Additionally, "nonswellable" hydrogel exhibited no mechanical hysteresis against a repetitive deformation and endured a compressive stress up to 60 MPa.

CONCLUSIONS: Our results demonstrate that the swelling suppression of hydrogels helps maintain their initial shape and mechanical properties under physiological conditions [2].

REFERENCES: ¹P. J. Flory (1953) *Principles of polymer chemistry*, Cornell University Press. ² H. Kamata, et al. (2014) *Science* **343**(6173):873-875.

ACKNOWLEDGEMENTS: This template was modified with kind permission from eCM Journal.



A novel bioink based on thermo- and photo-triggered tandem gelation for cartilage engineering

Matti Kesti¹, Michael Müller¹, Jana Becher³, Matthias Schnabelrauch³, Matteo D'Este², David Eglin², Marcy Zenobi-Wong¹

¹ Cartilage Engineering + Regeneration, ETH Zürich, Zürich, Switzerland. ² AO Research Institute Davos, Davos, Switzerland. ³ Biomaterials Department, Innovent e.V., Jena, Germany.

INTRODUCTION: Bioprinting is an emerging technology for fabricating tissue engineered grafts. **Bioprinters** replacement for prototyping purposes are well developed; however, there is still a lack of suitable biologically relevant printing materials, so called bioinks. The ideal bioink for extrusion printing should be initially liquid to allow for mixing with other polymers, peptides or cells and show a flow behavior suitable for the extrusion process (shear thinning). The final construct should be a stable, irreversibly crosslinked hydrogel with similar mechanical properties to the surrounding tissue. We have developed a bioink suitable for bioprinting with high cell viability. This bioink utilizes a tandem gelation process with a transient initial crosslinker and photocrosslinked biopolymer forming an interpenetrating network.

METHODS: Hyaluronan grafted isopropylacrylamide) (HA-pNIPAAM) was used as the thermoresponsive element of the bioink mixed with methacrylated hyaluronan to improve the mechanical properties of the final gel and to include biological cues. Rheological analysis of the bioink was used to identify the effect of embedded cells in the bioink. Cell encapsulated scaffolds were printed with a 300µm needle on a heated substrate (37°C) and after 10s UV exposure of each layer a final thickness of 2.8mm was achieved. Elution of the reversibly crosslinked, transient HA-pNIPAAM structure was performed in PBS at 4°C for 30 minutes. Chondrocyte viability was assessed with a MTS assay and live/dead assay 4 days after encapsulation.

RESULTS: Rheology measurements of the tandem crosslinked biopolymer hydrogel showed fast gelation in both thermo- and photo-triggered crosslinking reactions with a 8.4kPa storage modulus when cells were incorporated. Furthermore, the bioprinted structures were stable after photocrosslinking with good resolution as shown in the Figure 1. After the HA-pNIPAAM was eluted, the structures maintained their shape and became transparent. The cell viability data

presented in Figure 2 shows high viability in both assays. In the MTS assay the printed scaffold viability was 91.6% of the positive control.

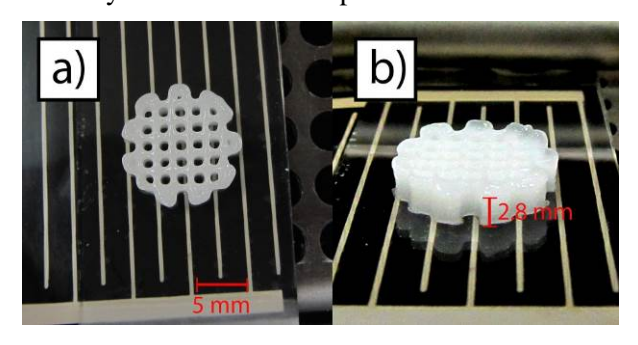


Fig. 1: Illustration of 3D printed scaffolds having a line thickness of 210µm and width of 620µm.

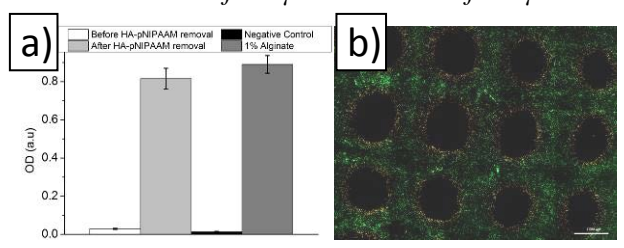


Fig. 2: Cell viability data 4 days after the printing a) MTS assay and b) live/dead assay.

DISCUSSION & CONCLUSIONS: In order to create a more open, porous network where nutrients and gas exchange can take place, HA-pNIPAAM was intentionally removed from the hydrogels. This step increased the cell viability from 3.3% to 91.6% of the positive control (Fig. 2a) after 4 days of encapsulation while providing a stable hydrogel structure. This bioink utilizes a tandem gelation process with a transient initial crosslinker to overcome the rheological limitations of pure biopolymer printing. This method can be used to facilitate 3D printing of biopolymer solutions which are otherwise not printable, thereby greatly expanding the range of bioink possibilities.

ACKNOWLEDGEMENTS: The work was funded by European Union Seventh Framework Programme (FP7/2007-2013) under grant agreement n⁰NMP4-SL-2009-229292 and by the Swiss National Science Foundation (CR32I3_146338/1).



Antimicrobial metals trapped in responsive systems

S. Kracht¹, K. M. Fromm¹

¹ Department of Chemistry, University of Fribourg, CH

INTRODUCTION: Today, many body implants consist of parts made of cobalt-chromium- or titanium-alloy and high molecular weight polyethylene parts. The high infection rates (\sim 5% for orthopaedic implants) [1] lead to increased suffering of the patient and enormous costs. While the metal parts can be already coated with antibacterial materials based on copper(II)^[2] or silver(I)^[3], incorporation of the latter into the polymer would also help lowering the infection rates due to a constant release of silver or copper over a prolonged time period.

Our ligand system is based on functionalized pyridine end-capped linker units which differ in the linkage unit and the nature of the linker chain, such as ethylene glycols or alkyl chains. Substitution on the pyridine rings offer the possibility to attach oligomers or polymer chains which can work e.g. as handles. By applying, for example, mechanical force, like ultra-sonication, the metal can be released by an external trigger and used for catalysis or in medicine, where its antimicrobial properties are requested.

RESULTS: A variety of different pyridine Schiff base ligands were synthesized and tested for their concentration dependent cytotoxicity against fibroblast cells. The cytotoxicity of the ligands changes depending on the length of the alkyl linker unit and the substitution position of the pyridine. If the length of the alkyl chain is between octyl and dodecyl, there was no toxic effect on fibroblast cells at low concentrations.

$$X = C,O, C/O$$

$$X = C,O, C/O$$

$$X = C,O, C/O$$

Scheme 1: General structure of the utilized pyridine imine and amine ligands.

Additionally, the imine functions were reduced with sodium borohydride to amines in order to

investigate the difference in cytotoxicity and complexation behavior.

The synthesized ligands were reacted with different copper(II) and silver(I) salts. The resulting complexes were tested for their antimicrobial activity against *E. coli*. Kirby-Bauer tests demonstrate the formation of inhibition zones for most of them, whereas the ligands alone do not show any antimicrobial properties.

Single crystal analysis reveals for example that the use of copper(II) bromide as starting material the formation of linear coordination polymers of copper(II), bridged by two bromide ions while the copper is also coordinated by the pyridine and the nearby imine function, which are in *cis*-position of two ligands. The alkyl chain is stretched out in these cases.

DISCUSSION & CONCLUSIONS: The pyridine imine ligands are accessible in a one-step reaction and in good yields. Reducing the imine functions is a potential second reaction step and nearly quantitative. Depending on the chain length, there is a concentration "window" in which the ligands are non-toxic.

The addition of copper(II) and silver(I) salts leads to the formation of various complexes. Crystal structures reveal the exact composition of these compounds and the accurate binding positions of the metal ions as well as the stoichiometry. The complexes show antimicrobial activity against *E. coli* as model gram-negative bacteria.

In the next steps, polymer handles will be attached to the existing ligand systems and the influence of this modification will be investigated.

REFERENCES: ¹R. O. Darouiche (2004), *N. Engl. J. Med.* **350**, 1422-1429. ² J. O'Gorman, H. Humphreys (2012), *J. Hosp. Infect.* **81**, 217-223. ³ S. Eckhard, P. S. Brunetto, J. Gagnon, M. Priebe, B. Giese, K. M. Fromm (2013), *Chem. Rev.* **113**, 4708-4754.

ACKNOWLEDGEMENTS: We thank the University of Fribourg, the NCCR for Bio-inspired stimuli-responsive materials and the FriMat for generous funding.



Modified polysaccharides for rapid microtissue formation: the QuickStick technique

C Millan¹, E Cavalli¹, P Ammann¹, A Häller¹, Y Yang², T Groth², K Maniura-Weber³, M Zenobi-Wong¹

¹ <u>Cartilage Engineering + Regeneration Lab</u>, ETH, Zürich, CH. ² <u>Biomedical Materials Group</u>, Institute of Pharmacy, Martin Luther University Halle-Wittenberg, DE. ³ <u>Materials-Biology</u> <u>Interactions Laboratory</u>, Empa, St. Gallen, CH

INTRODUCTION. Microtissues are quickly becoming a popular tool for studying cell behavior in biomimetic 3D environments. However, common methods for forming microtissues are time consuming and lack physiological relevance. Presented here is a new method called QuickStick in which modified polysaccharides are mixed in the presence of cells where they rapidly undergo crosslinking and form a robust microtissue. Here, we compare QuickStick microtissues and centrifuged micromass pellets as culture methods for inducing chondrogenesis of human MSCs.

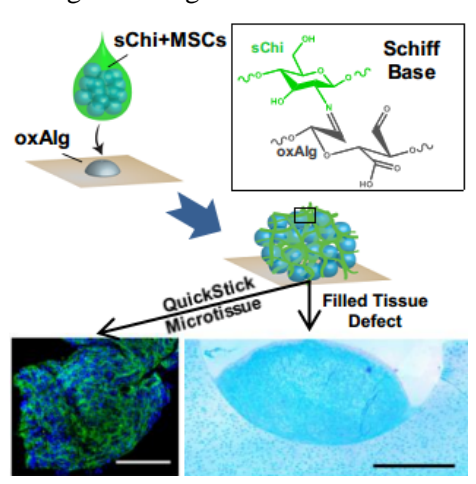


Fig. 1 Schiff base crosslinking between sChi containing MSCs and oxAlg entrap cells in a 3D network (bottom left, scale = 250um). Microtissues can also be used to fill cartilage tissue defects (bottom right, Alcian blue, scale = 1mm)

METHODS: For QuickStick (QS) microtissue formation (Fig. 1), human mesenchymal stem cells (MSCs) were suspended in a solution of N-succinyl chitosan (sChi) and mixed with droplets of oxidized alginate (oxAlg). In parallel, MSCs were centrifuged in conical well plates to form micromass pellets of the same cell number for comparison. Quantitative measures such as DMMB assay and RT-qPCR were used to compare chondrogenesis of MSCs in the two systems. GAG production and collagen deposition were

also visualized histologically. An explant defect model in bovine cartilage was developed for evaluating the potential of QS microtissues to produce de novo tissue in a simulated injury.

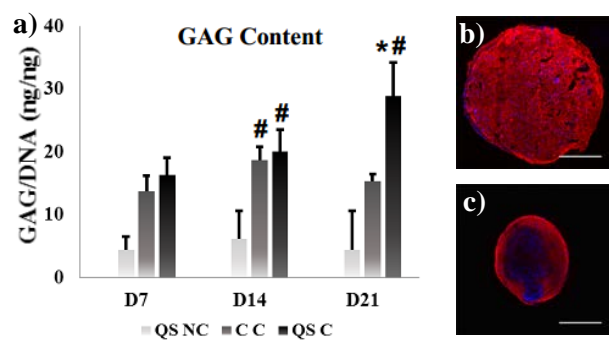


Fig. 2: a) GAG/DNA of QuickStick microtissues cultured in chondrogenic (QS C), non-chondrogenic media (QS NC), and centrifuged pellets in chondrogenic media (C C). b and c) Day 21 QuickStick (b) and centrifuged pellet (c) stained for type II collagen. Scale = 500µm.

RESULTS: After 21 days in chondrogenic media, QS microtissues had significantly higher production of cartilage markers than MSCs cultured in centrifuged micromass pellets. In QS microtissues, MSCs produced double the amount of GAG/DNA (Fig. 2a) with 30x and 22x higher expression of the genes type II collagen and aggrecan, respectively. Histology showed that MSCs in QS microtissues deposited more cartilage-like matrix and that the deposited proteins were more homogeneously distributed than in centrifuged pellets (Fig. 2b and 2c). In explant cartilage plugs, QS microtissues adhered and filled defects with de novo tissue rich in sulfated GAGs and type II collagen as confirmed by histology.

DISCUSSION & CONCLUSIONS: The novel QuickStick method is a promising tool for rapid microtissue fabrication, studying cell behaviors, and for replacing damaged tissue.

ACKNOWLEDGEMENTS: This work was supported by the Swiss National Science Foundation (CR3213_146338/1) and FP7 "Find & Bind" (NMP4SL2009229292).



Nanoencapsulation of silver-based antimicrobial drugs for biomaterial applications

J Gagnon¹, MJD Clift², A Petri-Fink², B Rothen-Rutishauser², KM Fromm¹

**I Fromm Group*, Department of Chemistry, University of Fribourg, CH. ** BioNanomaterials*

Research Group*, Adolphe Merkle Institute, University of Fribourg, CH.

INTRODUCTION: Implant-related infections still remain an issue in medicine especially due to the increased resistance of bacteria to antibiotics. 1 Many researchers are therefore turning to silver (Ag) drugs to prevent such infections. However, such drugs may be too soluble, thus becoming detrimental to the homeostasis of host cells,² thus their antimicrobial shortening Encapsulation of silver drugs is proposed as an advantageous technique in order to increase their stability and biocompatibility. In this project, silver-containing ceria nanocapsules (AgNP/CeO₂ NCs) were synthesized and were tested for their silver release. antimicrobial activity and cytotoxicity.

METHODS: AgNP/CeO₂ NCs were synthesized according to Figure 1. First, polystyrene beads were synthesized by emulsion polymerization. Then silver nanoparticles were produced by hydrogenation and encapsulated into the beads by sonication. The Ag-containing beads were coated with ceria by a sol-gel process. Finally, the polystyrene was removed by calcination.

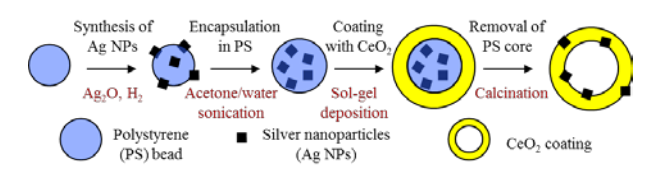


Fig. 1: Synthesis of AgNP CeO₂ NCs.

RESULTS: The obtained NCs were composed of ceria and silver, as determined by PXRD (data not shown). AgNPs are visible on SEM images (Figure 2) on the surface as well as in the cavity of AgNP/CeO₂ NCs.

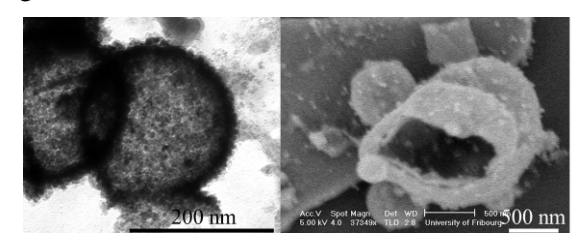


Fig. 2: TEM (left) and SEM (right) images of AgNP/CeO₂ NCs.

This system can release silver during a period exceeding 3 months as determined by ICP-OES (data not shown). Measurements of the ability for the CeO₂ NCs and AgNP/CeO₂ NCs to elicit a cytotoxic effect (LDH assay) upon mammalian lung barrier cells (A549) found increasing cytotoxicity in the presence of AgNP/CeO₂ NCs over a 7 day period (Figure 3). These NCs also demonstrated good antimicrobial activity against *E. coli* using agar diffusion test (data not shown).

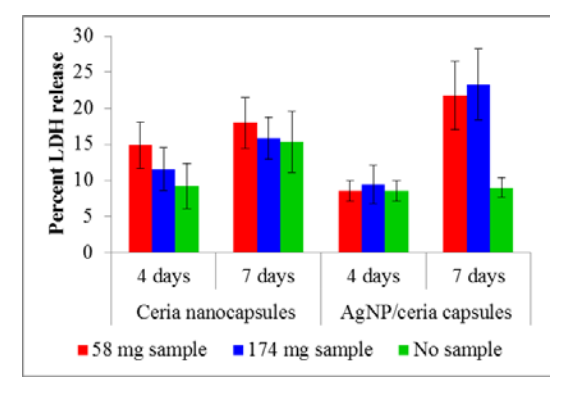


Fig. 3: LDH assay of CeO_2 and $AgNP/CeO_2$ NCs.

DISCUSSION & CONCLUSIONS: AgNP/CeO₂ NCs were successfully synthesized. AgNPs are integrated within the ceria shell, which enables a remarkably slow silver release. Cytotoxicity tests suggest that both CeO₂ and AgNP/CeO₂ NCs have a low cytotoxicity. A slight increase in LDH release was observed after 7 days of incubation for AgNP/CeO₂ NCs. AgNP/CeO₂ NCs also demonstrated a good antibacterial activity. These NCs therefore offer an advantageous strategy towards preventing implant-related infections.

REFERENCES: ¹ P. Gilbert, P.J. Collier, M.R.W. Brown (1990) *Antimicrob. Agents Chemother.*, **34**: 1865. ² S. Hackenberg, A. Scherzed, M. Kessler, S. Hummel, A. Technau, K. Froelich, C. Ginzkey, C. Koehler, R. Hagen, N. Kleinsasser (2011) *Toxicol. Lett.*, **201**: 27.

ACKNOWLEDGEMENTS: We are grateful to the Swiss National Science Foundation, the University of Fribourg, FriMat and the Adolphe Merkle Foundation for generously supporting this project.



Ni release from rapid prototyped 3D NiTi scaffolds

W Hoffmann^{1,2}, T Bormann^{2,3}, A Kessler², D Wendt¹, M de Wild²

¹ Institute for Surgical Research and Hospital Management, University Hospital Basel, Basel, Switzerland ² University of Applied Sciences Northwestern Switzerland, School of Life Sciences, Institute for Medical and Analytical Technologies, Muttenz Switzerland, ³ Biomaterials Science Center, University of Basel, Switzerland.

INTRODUCTION: The shape memory alloy nickel-titanium is a promising biomaterial for loadbearing implants, exhibiting pseudo-elastic behavior and allowing for mechanical stimulation of adherent cells and adjacent tissues, thus improving the osseo-integration. For a metal, NiTi has a low elastic modulus minimizing the effect of stress-shielding.2 However, Ni release from NiTi implants remains a significant concern as its toxic effects have been linked to increased levels of oxidative stress found within cells.³ With the ultimate goal of fabricating porous implants intended for load-bearing sites, NiTi substrates were fabricated by means of selective laser melting (SLM), and the release of Ni ions was assessed.

METHODS: Fig. 1 represents a NiTi scaffold built by means of SLM (Realizer 100, SLM-Solutions, Germany) using NiTi powder (Memry GmbH, Germany). To mimic physiological loading conditions, uniaxial dynamic compression was applied toscaffolds using a servo-hydraulic testing machine (walter+bai AG, Switzerland) with a sinusoidal loading profile, 100 µm displacement amplitude and a frequency of 8 Hz. During the loading cycles, Ni release from NiTi scaffolds was supported via continuous, recirculating perfusion with PBS solution (0.3 ml/min). Samples for Ni release measurements were taken at 24h (690'000 cycles), 1 week (4.8x10⁶ cycles) and 2 week time points (9.6x10⁶ cycles). The Ni amount was assessed by atom absorption spectroscopy (AAS, Perkin Elmer, AAnalyst 800, graphite furnace, 232 nm).

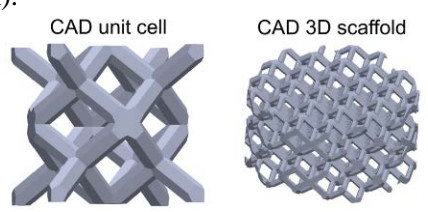


Fig. 1: CAD illustration of the unit cell and the cylindrical SLM-NiTi scaffold (4 mm height and 8 mm diameter).

RESULTS: The AAS measurements reveal Ni release in both loaded and unloaded conditions.

The mechanically loaded NiTi scaffolds demonstrated a significantly higher Ni release within the first 24h. Thereafter only small, time-dependent increases were detected. However, at all time points, the levels of released Ni ions were below the cytotoxic level for fibroblastic cells.⁴

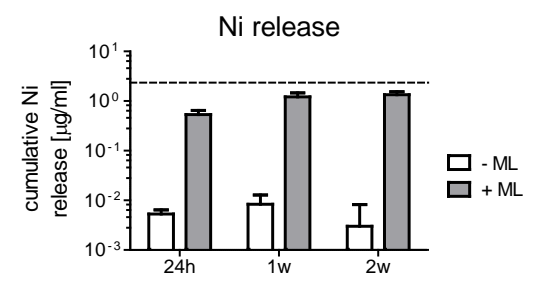


Fig. 2: Cumulative Ni release for unloaded (-ML) and loaded (+ML) NiTi scaffolds. Dashed line depicts cytotoxic Ni ion level⁴.

DISCUSSION & CONCLUSIONS: Unloaded SLM NiTi constructs show minimal Ni ion release. Upon application of physiological loads, cracks may form in the titanium oxide layer on the NiTi surface. Due to the rupture of the protective oxide layer, Ni ions are released into the perfusate. The Ni concentrations determined in this study remain under the cytotoxic level of 2.35 μg/mL⁴. Surface treatments could further improve the inertness of NiTi constructs. Moreover, under in vivo conditions, NiTi implants are continuously flushed by the bloodstream minimizing local Ni ion concentrations even further. Furthermore, MSC have been shown to colonize loaded SLM-NiTi scaffolds with no signs of cytotoxic effects⁵.

REFERENCES: 1. Bormann *et al.*, Acta Biomater 10(2):1024-34, 2014. 2. de Wild. *et al.*, J Mater Eng Perform (*in press*), 2014. 3. Plant *et al.*, Biomaterials 26 (2005) 5359-5367. 4. Taira *et al.*, J Oral Rehabil. 2000;27(12):1068-72. 5. Habijan *et al.*, Acta Biomater. 2011 Jun;7(6):2733-9

ACKNOWLEDGEMENTS: We sincerely thank MEMRY GmbH, Weil am Rhein, Germany, for powder and knowledge supply. The financial support of the Swiss National Science Foundation within the research program NRP 62 'Smart Materials' is gratefully acknowledged.



Hydrophobic gentamicin loaded poly(trimethylene carbonate) delivery system for the treatment of orthopaedic infections

GA ter Boo^{1,2}, DW Grijpma², RG Richards¹, TF Moriarty¹, D Eglin¹

¹ AO Research Institute Davos, Davos Platz, CH. ² Department of Biomaterials Science and Technology, University of Twente, Enschede, NL. gert-jan.terboo@aofoundation.org

INTRODUCTION: Infection is one of the main threats limiting the success of modern-day orthopaedics and traumatology. Certain strains of bacteria (e.g.Staphylococcus *aureus*) are able to invade and survive within osteoblasts[1], seriously complicating treatment. Extended release and possibly intracellular targeting could be obtained by hydrophobic modification of gentamicinsulphate (GEN-SULPH). Poly(trimethylene carbonate) (PTMC) was chosen as carrier, as it degrades by surface erosion without acidic degradation products that impair antibiotic action or bone regeneration.

METHODS: Gentamicin-AOT preparation: Docusate sodium (AOT) was used for hydrophobic ion-pairing with GEN. Equal volumes of GEN-SULPH solution in buffer (10mM sodium acetate, KCl and CaCl₂ (pH 5) (0.40 w/v%) and AOT in DCM (1.25 w/v%) were mixed by vigorous stirring for 3h and left for 0.5h to separate the 2 phases. GEN-AOT was isolated from the DCM. Viability of human fibroblast cell line upon antibiotic exposure: A cell titer blue assay was used to assess the effect of GEN-AOT on cellviability. hTERT fibroblast BJ-1 cells were used to determine the viability after 24h and 72h by measuring the fluorescence intensity. Antimicrobial susceptibility testing: selected strains were: S. aureus NCTC 12973 (SA) and S.epidermidis 103.1 (SE). Antibiotic solutions were prepared in Cation adjusted Mueller Hinton broth, in a concentration range of $0.06 - 256 \,\mu\text{g/ml}$ for GEN-SULPH. For AOT and GEN-AOT a concentration range was prepared reflecting the same molar concentrations prepared for GEN-SULPH. Minimum inhibitory (MIC) and minimum (MBC) concentrations bactericidal determined according NCCLS M7-A5 guidelines for bacteria that grow aerobically. Preparation of **GEN-AOT loaded PTMC:** For the preparation of monodisperse antibiotic loaded poly(trimethylene carbonate) (PTMC) and Poly(D,L-lactide) (PDLLA) (control) microspheres (MSs) $microsieve^{TM}$ emulsification technology of Nanomi monosphere technology (The Netherlands) was used. GEN-AOT loaded MSs

were prepared by adding 20% GEN-AOT to a 1% PTMC solution. Ø 8 mm PTMC discs with 10% GEN-AOT were prepared as well (not shown).

RESULTS: High concentration of GEN-SULPH antibiotic did not impair fibroblast viability. GEN-AOT reduced viability with ~50% at 11x10⁻⁶M (fig. 1)

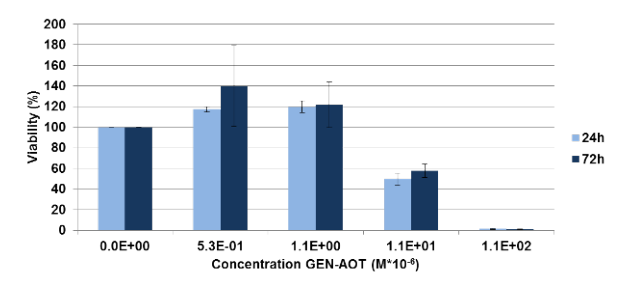


Fig 1. hTERT fibroblast viability

Both GEN-SULPH and GEN-AOT antibiotics inhibit staphylococci at equal molar concentration (2.1x10⁻⁶M (SA) and 0.5x10⁻⁶M (SE)). GEN-AOT is bactericidal for SE at lower concentration (0.5x10⁻⁶M) than GEN-SULPH (4.2x10⁻⁶M).

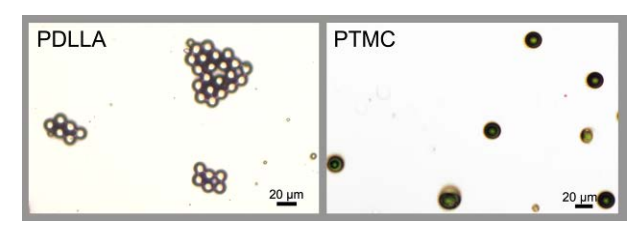


Fig 2. PTMC (r) and PDLLA (l) MSs prepared by microsieve emulsification

DISCUSSION & CONCLUSIONS: GEN-SULPH and GEN-AOT both inhibit SA and SE at equal molar concentrations. Cellular uptake of GEN-AOT is reflected by lowered cell viability. Studies are ongoing to investigate the release and bactericidal efficacy of GEN-AOT loaded MSs.

REFERENCES: ¹J.K. Ellington, et al (2006) *J Orthop Res.* **24**: 87-93

ACKNOWLEDGEMENTS: Microsieve TM emulsification equipment was kindly provided by Nanomi monosphere technology (The Netherlands) and TMC monomer by Huizhou Foryou Medical Devices (China).



Dissolution of CaCl₂ loaded into beta tricalcium phosphate porous blocks

D Alexeev¹, B Andreatta¹, M Bohner¹

**IRMS Foundation, Switzerland.

INTRODUCTION: Porous CaP ceramics are widely used as bone substitute material as well as for bone tissue engineering. There have been many studies aimed at loading the open porous surface of the ceramic with various therapeutic compounds. Calcium phosphate compounds have been arguably shown to be osteoinductive on their own [1]. It is then possible that the cell response can be guided by release of phosphate and calcium ions.

The aim of the present work is to investigate the possibility of loading CaP with additional Ca and PO_4 ions and to study the release mechanics as well as the parameters that might influence it. β tricalcium phosphate (β -TCP) has been chosen as a matrix material with well-known biocompatibility and clinical applications [2].

METHODS: Three types of sintered porous β-TCP samples were prepared from cement produced by reacting α-TCP with water. Macroprous blocks were obtained through emulsification process [2] and sintered at 900 °C for 1 hour and machined thereafter. Microporous blocks were sintered at 1250 °C for 4 hours and also machined. Finally microporous blocks were sintered at 1000 °C for 4 hours.

Samples were calcined at 500 °C, followed by impregnation with CaCl₂ 10 M solution, using capillary forces. Samples were then dried at 110 °C in vacuum.

The dissolution of the salt was studied submerging the samples in 250 mL of ultrapure water. Periodic 1mL samples of the solution were taken at times up to 24 hours. The solution samples were then analysed using ion coupled plasma mass spectrometry to determine Ca²⁺ and PO₄³⁻ content.

The data was fitted using Peppas and Ritger equation [3] for diffusion controlled release from porous cylinder.

RESULTS & DISCUSSION: The fitting of experimental data established that the release of salt is diffusion controlled.

The Peppas function was a good fit at early times (Figure 1). A deviation from diffusion function was observed at longer dissolution times, where a

second sustained dissolution mode emerged. The reason for it could be due to presence of nanoporosity or adsorption of calcium to ceramic surface. Scaffold dissolution can be excluded from possible causes as blank controlled samples showed significantly lower release.

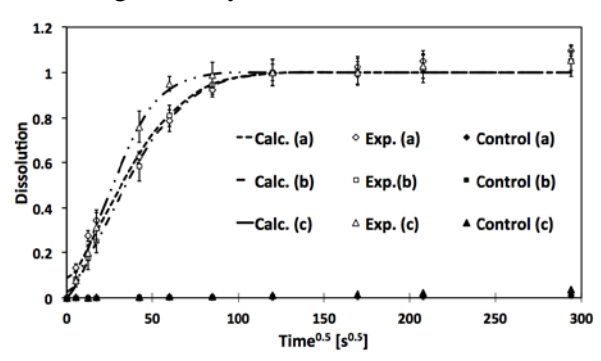


Figure 1. Ca ions dissolved from (a) machined macroporosu, (b) machined microporous, (c) not machined microporous samples.

Table 1. Values calculated using extended Peppas equation, error with respect to experimental data.

Sample Type	Diffusion [cm ² /s]	Standard Error	R ²
Macroporous	6.22e-05	15.6%	0.98
Microporous	6.11e-05	6.08%	0.99
Non-machined	1.11e-04	6.67%	8
Microporous			0.99
			8

CONCLUSIONS: The feasibility of loading CaP ceramics with salts and the subsequent release was confirmed. However the release is not adequate for biological application as it might be too fast. Furthermore the dissolution profile in vivo remains to be investigateed.

REFERENCES: ¹H Yuan, M Van Den Doel, JD De Bruijn (2002), J. of Mat Sci: Materials in Medicine, 13(12):1271-1275. ²M. Bohner (2001), Key Eng. Mat., 192-195:765-768. ³P. L. Ritger, N.A. Peppas (1987), Journal of Controlled Release, 5(1):23-36.



Short-term co-delivery of fibrin-bound VEGF and PDGF-BB proteins ensures normalization and stabilization of VEGF-induced angiogenesis

V Sacchi¹, MM Martino², R Gianni-Barrera¹, JA Hubbell², A Banfi¹

¹ Department of Surgery, Basel University Hospital and Department of Biomedicine, University of Basel, Switzerland. ² Institute of Bioengineering, EPFL, Lausanne, Switzerland

INTRODUCTION: Therapeutic angiogenesis is required both for rapid vascularization of tissue engineered constructs and to treat ischemic conditions. Vascular endothelial growth factor (VEGF) is the master regulator of angiogenesis and its therapeutic potential depends on both its dose and duration of expression. VEGF delivery for at least 4 weeks is required to avoid regression of induced vessels, but sustained and uncontrolled expression can cause angioma growth [1]. Hence, both avoidance of angiomas and rapid stabilization of newly induced vessels with short-term treatments are required to ensure safety and efficacy. In a gene therapy approach, we found that co-expression of the maturation factor Platelet derived growth factor-BB (PDGF-BB) can prevent aberrant angiogenesis by uncontrolled VEGF levels [2]. Here we tested the hypothesis that delivery of recombinant VEGF and PDGF-BB proteins from a state-of-the-art matrix-bound system, based on transglutaminase (TG) reaction to bind the modified factors into fibrin hydrogels [3], can both prevent aberrant angiogenesis by VEGF and ensure rapid stabilization despite shortterm treatment.

METHODS: The transglutaminase substrate sequence NQEQVSPL (α_2 -PI₁₋₈) was fused to mouse VEGF₁₆₄ and PDGF-BB (TG-factors), to allow their covalent cross-linking into fibrin hydrogels and release only by enzymatic cleavage [3]. Gels carrying different doses of TG-VEGF, TG-PDGF-BB, both together or no factors (control) were injected in limb muscles of SCID mice. Vascular morphology, quantity and stabilization were analyzed after 2 weeks and 2 months.

RESULTS: We previously determined the dose-dependent effects of increasing doses of TG-VEGF alone delivered from fibrin hydrogels [4]. Here we found that: 1) fibrin gels were completely degraded in 10 days in all conditions; 2) by 2 weeks, co-delivery of TG-PDGF-BB completely normalized aberrant angiogenesis induced by 2 different high doses of TG-VEGF alone (25 and 50 μ g/ml), yielding instead only mature capillary

networks that were all functionally perfused by systemic circulation; 3) normalization achieved with a wide range of PDGF-BB:VEGF ratios from 1:3 to 1:20. A ratio 1:20 was used for further investigations; 4) co-delivery of PDGF-BB with a VEGF dose inducing only normal angiogenesis (5 µg/ml) caused a moderate homogeneous increase in vessel diameter, which may be therapeutically advantageous, but no change in vessel quantity compared to VEGF alone; 5) 10 days of co-delivery of PDGF-BB with both low and high VEGF doses (5 and 50 µg/ml) caused complete stabilization and persistence of induced vessels still after 2 months, whereas 50% and 75% regressed with low and high VEGF alone, respectively (Fig. 1).

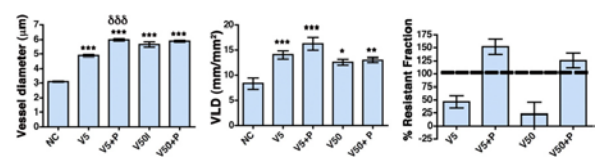


Fig. 1. Diameter, quantity (VLD) and stabilized fraction of vessels induced by low (V5) and high (V50) doses of VEGF alone or with PDGF-BB.

DISCUSSION & CONCLUSIONS: Controlled co-delivery of TG-VEGF and TG-PDGF-BB proteins provides a convenient (off-the-shelf) and clinically applicable approach to: 1) expand the therapeutic range of VEGF doses; and 2) rapidly stabilize newly induced vessels with only 10 days' treatment and avoiding genetic modification.

REFERENCES: ¹ C.R. Ozawa, A. Banfi, N.L. Glazer, et al (2004) *J Clin Invest.* **113**:516-27. ² A. Banfi, G. von Degenfeld, R. Gianni-Barrera, et al (2012) *FASEB J.* **26**:2486-97. ³ J.C. Schense, J. Bloch, P. Aebischer, et al (2000) *Nat. Biotechnol.* **18**:415-19. ⁴ V. Sacchi, R. Mittermayr, J. Hartinger, et al (2014) *Proc. Natl. Acad. Sci. U.S.A.* in press.

ACKNOWLEDGEMENTS: This work was supported by Swiss National Science Foundation grants 127426 and 143898 to A.B. and EU FP7 grant ANGIOSCAFF (214402) to A.B. and J.A.H.



Bioactive scaffolds releasing collagen-binding neurotrophic factors (NTFs) for axonal growth and guidance

M Reggane¹, B Gander¹, S Madduri¹

¹Department of Chemistry and Applied Biosciences, ETH Zürich, CH.

INTRODUCTION: Peripheral nerve injuries affect more than one million people each year and often result in life-long disabilities. Development of bioactive scaffolds with topographical guidance and sustained neurotropic factors (NTFs) support may address some of the limitations associated with presently available treatment modalities, i.e., nerve grafting and artificial nerve conduits (NCs)¹. This study aimed at investigating two approaches to tailor the release of glial cell line-derived neurotrophic factor (GDNF). For this, we have engineered GDNF with collagen binding domain (CBD-GDNF) which was released from two delivery systems i.e., collagen NC scaffolds and PLGA microfibrous scaffolds respectively. Later approach was envisaged to integrate the PLGA guidance fibers into collagen NC.

METHODS: Recombinant CBD-GDNF was cloned into eukaryotic vector pCDNA3, expressed in mammalian 911 cell line and purified by immobilized metal affinity chromatography. Recombinant CBD-GDNF or native GDNF (50 ng/NC) was loaded into collagen NCs fabricated by spinning mandrel technology. For the other approach, PLGA solution was premixed with these growth factors (5ng/mg) and fabricated into aligned or random microfibrous scaffolds. Release kinetics were studied in vitro over 28 days from both collagen NC and PLGA scaffolds. Bioactivity of released NTFs was assessed by using Neuro-2A cell line. Furthermore, the ability of bioactive PLGA microfibrous scaffolds to promote axonal outgrowth was tested in vitro using chicken embryonic dorsal root ganglionic (DRGs) explant cultures².

RESULTS: Collagen NC scaffolds showed sustained release for both GDNF and CBD-GDNF over 28 days (Fig. 1). Interestingly, CBD-GDNF mediated slow and low release with significantly reduced initial burst release when compared to native GDNF. Other approach using PLGA scaffold also resulted in sustained release of growth factors, but the release profiles were similar for both GDNF and CBD-GDNF. The release rates were nearly constant over 28 days with only few picograms of daily release. Bioactivity of released NTFs was maintained throughout the entire release period as demonstrated by neuronal differentiation

of Neuro-2A cells treated with NTFs release. Topography of the microstructed PLGA scaffold releasing NTFs determined the direction and extent of axonal outgrowth from DRG explants. Axonal outgrowth from DRGs was perfectly (99%) in line with the aligned fibers, but randomly oriented on non-aligned fibers (Fig. 2).

DISCUSSION&CONCLUSIONS:

Immobilization of NTFs in collagen NCs by fusion with collagen-binding domain is an appealing strategy for controlling release kinetics with reduced burst release and for sustaining bioactivity of NTFs.

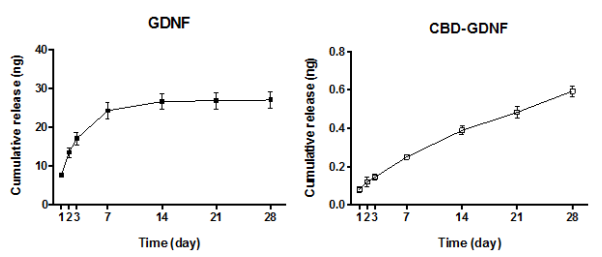


Fig. 1: Cumulative release of GDNF and CBD-GDNF from collagen NCs over 28 days.

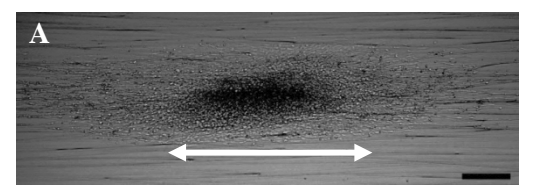




Fig. 2: Axonal growth on aligned (A) and random fibers (B) releasing NTFs; Arrow indicates direction of axonal growth. Scale bar indicates 0.5 mm

Alternatively, electrospun PLGA microfibers appeared to be appropriate delivery system for sustaining NTFs' slow release and holds potential interest for guiding the peripheral axonal regeneration. Future studies will assess the beneficial effects of collagen NC integrated with GDNF-PLGA microfibers in rat nerve gap model.

REFERENCES: ¹S. Madduri et al (2010a) *Biomaterials* **31**: 2323-34. ²E. Stoeckli et al (1991) *J cell Biol* **112**: 449-55

ACKNOWLEDGEMENTS: We acknowledge the enabling financial support by SNSF.



Proliferation of ASC-derived endothelial cells in a 3D electrospun mesh: Impact of bone-biomimetic nanocomposite and co-culture with ASC-derived osteoblasts

S Gao¹, M Calcagni², Manfred Welti², Sonja Hemmi¹, Nora Hild³, WJ Stark³, G Meier Bürgisser², GA Wanner¹, P Cinelli¹, J Buschmann²

¹ Trauma Surgery, University Hospital Zurich, CH. ² Plastic and Hand Surgery, University Hospital Zurich, CH. ³Institute for Chemical and Bioengineering, Department of Chemistry and Applied Biosciences, ETH Zurich, CH.

INTRODUCTION: Fractures with a critical size bone defect are associated with high rates of delayed- and non-union. The treatment of such complications remains a serious issue in orthopaedic surgery. Adipose derived stem cells (ASCs) combined with biomimetic materials can potentially be used to increase fracture healing. Nevertheless, a number of requirements have to be fulfilled: particular the vascularization of the bone constructs¹. Here, the objectives were to study the impact of ASCderived osteoblasts on ASC-derived endothelial cells in a 3D co-culture and the effect of 40 wt % of amorphous calcium phosphate nanoparticles on the proliferation and differentiation of ASCderived endothelial cells when present in PLGA.

METHODS: Five primary ASC lines were differentiated towards osteoblasts (OB) and endothelial cells (EC) and two of them were chosen based on quantitative PCR results. Either a mono-culture of ASC-derived EC or a co-culture of ASC-derived EC with ASC-derived OB (1:1) was seeded on an electrospun nanocomposite of poly-(lactic-co-glycolic acid) and amorphous calcium phosphate nanoparticles (PLGA/a-CaP; reference: PLGA). The proliferation behavior was determined histomorphometrically in different zones and the expression of von Willebrand Factor (vWF) was quantified.

RESULTS: Independently of the fat source (biologic variability), ASC-derived osteoblasts decelerated the proliferation behavior of ASCderived endothelial cells in the co-culture compared to the mono-culture. However, expression of vWF was clearly stronger in the coculture, indicating further differentiation of the ASC-derived EC into the EC lineage. Moreover, the presence of a-CaP nanoparticles in the scaffold slowed the proliferation behavior of the co-culture cells, too, going along with a further differentiation of the ASC-derived OB, when compared to pure PLGA scaffolds.

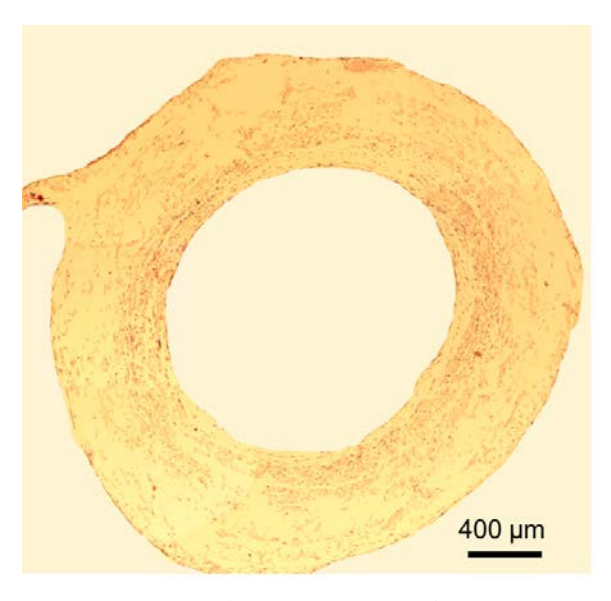


Fig. 1: Hematoxylin&Eosin stained cross-section of a co-culture of ASC-derived OB and ASC-derived EC seeded on a PLGA/a-CaP nanocomposite tube.

DISCUSSION & CONCLUSIONS: This study revealed significant findings for bone tissue-engineering. Co-cultures of ASC-derived EC and ASC-derived OB stimulate each other's further differentiation. A nanocomposite with a-CaP nanoparticles offers higher mechanical stability, bioactivity and osteoconductivity compared to mere PLGA and can easily be seeded with predifferentiated EC and OB.

REFERENCES: ¹ M.W. Laschke, Harder Y., Amon M., Martin I., Farhadi J., Ring A., Torio-Padron N., Schramm R., Rucker M., Junker D. et al. (2006) *Tissue Engineering* **12(8)**:2093-2104.

ACKNOWLEDGEMENTS: We thank Miss Pia Fuchs for her help with the histology.



Assessment of bone grafting materials in oral surgery

Simone E. Hieber¹, Anja K. Stalder¹, Bernd Ilgenstein¹, Natalia Chicherova¹, Hans Deyhle¹, Felix Beckmann², Stefan Stübinger³, Brigitte von Rechenberg³, and B. Müller¹

¹ <u>Biomaterials Science Center</u>, University of Basel, Switzerland, ² <u>Helmholtz-Zentrum Geesthacht</u>, Institute of Materials Research, Geesthacht, Germany, ³ <u>Center for Applied Biotechnology and Molecular Medicine</u>, University of Zurich, Switzerland

INTRODUCTION: The efficacy of bone grafting materials is generally assessed on the basis of histological evaluations. In the present study three augmentation materials were analyzed by a combination of micro computed tomography (μ CT) and histology. The registration of the two-dimensional histological slices with their counterpart from the three-dimensional μ CT data set was performed manually and automatically. It allowed the compilation of a joint histogram.

METHODS: First, the extraction site was filled with easy-graftTM (Sunstar Degradable Solutions AG, Schlieren, Switzerland). Second, another bone defect was substituted with Bio-Oss® Block (Geistlich Biomaterials, Baden-Baden, Germany). Third, a vertical bone defect in the region of a molar was augmented first BoneCeramic® (Institute Straumann AG, Basel, Switzerland). To reveal the 3D morphology of the three specimens, synchrotron radiation-based tomography micro computed (SR_uCT) measurements were carried out at the HZG beamline W2 / DORIS III at DESY, Hamburg, Germany in the conventional absorption contrast mode at 25 keV photon energy and 2.2 µm pixel size. After the SRuCT analysis the three biopsies were further processed for histology. The combination of histological images and µCT data for the bone assessment requires the multi-modal mapping of 2D slices on 3D data sets. Due to the complexity of 2D-3D registration the present study followed manual and algorithmic approaches. The preparation of joint histograms included the nonrigid registration of the selected 2D images. The entries of the 2D joint histogram represent the number of pixels within the physical absorption intervals of the µCT slice and the color values of the corresponding histological slice.

RESULTS: After the healing period, sufficient bone was offered to place the implant in all cases. Based on the histogram of the μ CT data sets the amount of bone, augmentation material and soft tissue was determined. In the first specimen we found 1.3 % easy-graftTM, 34.1 % bone, and

64.6 % embedding material, which also includes the soft tissue components. The second specimen included 57 % soft tissue and embedding, 14.2 % bone, 25.7 % Bio-Oss®, the third one contained 45.5 % soft tissue and embedding, 4.7 % BoneCeramic® and 48.9 % bone. The joint histogram revealed anatomical structures such as the early-formed bone. It allowed for the identification of anatomical features, which can neither be extracted from histology nor from μCT data alone.

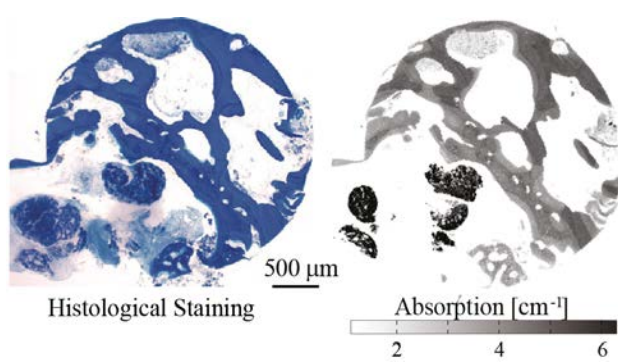


Fig. 1: Histological slice (left) and the corresponding μ CT image (right) registered from the 3D data set for the biopsy containing easy-graftTM (Sunstar Degradable Solutions AG, Schlieren, Switzerland).

DISCUSSION **CONCLUSIONS:** & The combination of SRuCT and selected histological sections provides a detailed quantitative view of morphology and maturation. bone The combination of the techniques leads to insights, not delivered by one method alone. To this end, SRµCT and histology are complementary methods to assess the bone quality, including bony tissues formed as the result of augmentation materials.

REFERENCES: ¹A. Stalder et al. (2014) Combined use of micro computed tomography and histology to evaluate the regenerative capacity of bone grafting materials Int J Mater Res **105** online ²B. Ilgenstein et al. (2012) Combined micro computed tomography and histology study of bone augmentation and distraction osteogenesis Proc SPIE **8506**: 85060M



Adipose-derived stromal cells form bone through endochondral ossification

R Osinga¹, N di Maggio², N Allafi¹, A Barbero², DJ Schaefer¹, I Martin², A Scherberich²

¹Department of Plastic, Reconstructive, Aesthetic and Hand Surgery, University Hospital of Basel

²Laboratory of Tissue Engineering, Department of Surgery, University Hospital of Basel and

Department of Biomedicine, University of Basel, Basel, Switzerland

INTRODUCTION: Bone marrow derived stromal cells (BMSC) can form bone ectopically either through intramembranous ossification, by direct mineralization of the BMSC-laid matrix, or through endochondral ossification, by forming cartilaginous matrix which is remodelled into bone. Adipose-derived stromal cells (ASC), which have a lower osteogenic capacity compared to BMSC, have only been shown to form bone through intramembranous ossification. The goal of this study was i) to investigate if ASC can form bone through endochondral ossification and ii) to determine which culture conditions are required to promote differentiation of ASC towards an endochondral route.

METHODS: In a preliminary study, pellets were formed as follows. Stromal vascular fraction (SVF) from human adipose tissue was obtained from three healthy donors and cultured in monolayer in the presence of FGF-2 to allow ASC expansion. At 90% confluency, micromass pellets were generated by centrifugation and cultured in serum free medium in the presence of TGFb-3, dexamethasone, ascorbic acid and BMP-6 for 4 weeks to promote chondrogenic differentiation. Half of the pellets were cultured for additional 2 weeks in serum free medium lacking TGFb-3 and supplemented BMP-6, but glycerophosphate, 1-thyroxin and Il1b, to actively induce hypertrophic differentiation. All constructs were implanted subcutaneously into nude mice and harvested after 4 and 8 weeks, followed by histological and immunohistochemical analysis. Based on these results, frozen SVF of the donor with the greatest chondrogenic potential was again expanded as described above. At 90% confluency, cells were seeded on 4 mm-diameter, 1 mm-thick collagen-based cylindrical scaffolds (UltrafoamTM) and cultured for either 4 or 6 weeks in medium. After 4 weeks chondrogenic chondrogenic medium, hypertrophy was induced for 1 or 2 weeks, or omitted. All constructs were implanted subcutaneously into nude mice. harvested after 4 and 8 weeks and analyzed as described above.

RESULTS: After in vitro culture, both pellets and scaffolds showed deposition of cartilaginous matrix positive for glycosaminoglycans (GAG) and collagen type II. Upon active induction of hypertrophy, gene expression analysis showed upregulation of collagen type X, BSP and MMP13, which was also confirmed by immunohistochemistry staining.

In vivo, ASC formed bone tissue both in pellets and in scaffolds, with and without active induction of hypertrophy, but with different kinetics. In pellets, bone was already found after 4 weeks, whereas in scaffolds it could only be observed after 8 weeks. The constructs displayed areas still positive for GAG and collagen type II, containing chondrocytes. Adjacent areas showed the presence of osteocytes, surrounded by matrix expressing collagen type X, BSP and MMP13. Osteoclasts were found in the outer rim of the constructs, remodelling. indicating matrix hybridization for human-specific sequences revealed a significant contribution of implanted ASC in bone formation. This bone vascularized and included bone marrow at 8 weeks. These data altogether indicate that bone formation by human ASC occurred through endochondral ossification.

DISCUSSION & CONCLUSIONS: ASC were able to generate bone tissue via an endochondral program both in pellets and in collagen sponges. As in BMSC, active induction of hypertrophy was not mandatory. Adipose tissue contains a greater density of mesenchymal progenitor cells and is much easier to harvest than bone marrow. These features, combined with the ability to undergo endochondral ossification, make ASC an alternative to BMSC as a source of stromal cells in therapeutic approaches for bone regeneration.

ACKNOWLEDGEMENTS: This work was funded by the Swiss National Science Foundation (SNF grant #138519 to A.S. and I.M.).



Biomaterials functionalization by decoration with cell-laid extracellular matrices

P Bourgine¹, B Pippenger², S Piegeot¹, E Gaudiello³, T Klein¹, I Martin¹

¹Tissue engineering, ²Osteoarthritis Research Centre and ³Cell and gene therapy labs, University Hospital Basel, Switzerland.

INTRODUCTION: Inert materials used medicine regenerative require either association of living cells or the delivery of overphysiological doses of discrete growth factors to be biologically effective. As an alternative, materials can be functionalized through the decoration by extracellular matrix (ECM), acting as a physiological reservoir of multiple growth factors that - thanks to the suitable way of presentation – are effective at lower doses [1]. The generation of such materials coated with ECM ideally requires the use of standard cell lines to deposit a thick ECM and of a decellularization method allowing for both an efficient cell removal and the preservation of the ECM integrity. The concept of cell-free ECM coated grafts is here explored in the context of osteo-inductive and angiogenic graft engineering.

METHODS: Osteo-inductive grafts were generated using a death-inducible, immortalized human Mesenchymal Stromal Cell (hMSC) line [2], seeded on ceramic scaffolds (Engipore, Finceramica Faenza, Italy) and cultured for 4 weeks in osteogenic medium in a 3D perfusion bioreactor system (U-CUP, Cellec Biotek AG, Basel). The ECM was decellularized by supply of the apoptotic inducer directly in the 3D culture system. Grafts were implanted in a rat cranial defect model to assess their regenerative potential after 12 weeks. Angiogenic grafts were generated using the same protocol, but with a death-inducible cell line overexpressing VEGFa. The angiogenic performance of these VEGFa enriched ECM was assessed by subcutaneous implantation for 1 week in rat.

RESULTS: ECM coated ceramic materials were successfully generated in the 3D bioreactor culture (fig.1) and subsequently decellularized (fig.2). The apoptosis induction allowed for efficient decellularization while preserving the deposited matrix. These 'apoptized', cell-free, ECM decorated constructs induced enhanced bone regeneration or vessel formation as compared to the respective un-coated materials.

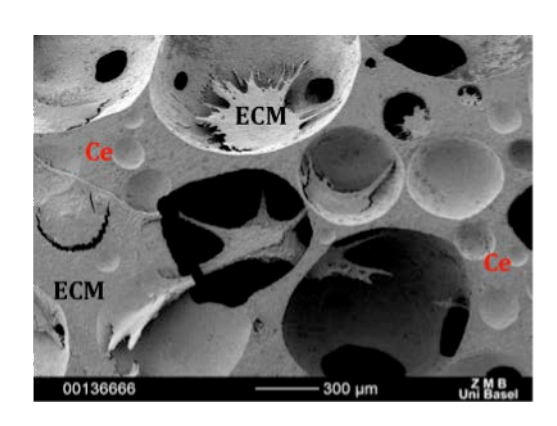
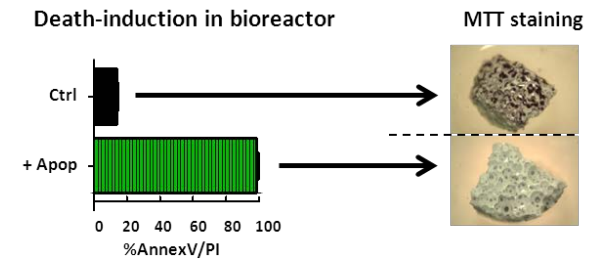


Fig. 1: Generation of extracellular matrix (ECM)



coating material (ceramic, Ce).

Fig. 2: Decellularization efficiency of ECM coated scaffold.

DISCUSSION & CONCLUSIONS: The use of death-inducible cell lines allowed for the generation of cell-free, ECM-coated materials. Moreover, the apoptotic decellularization was shown to preserve the ECM integrity. Thus, inert materials can be functionalized by the deposition of ECM, and further enriched in specific factors in order to enhance and customize their regenerative performance. The resulting implants could be used in a variety of clinical scenarios, as cell-generated but cell-free allograft substitutes capable to instruct tissue repair.

REFERENCES: ¹Bourgine P et al, Biomaterials. 34(26):6099, 2013, ² Bourgine P et al, Stem Cell Research

2014.

ACKNOWLEDGEMENTS: To the Marie curie foundation, FP7 and MultiTERM European program.



Characterizing the mechanical stability of antibacterial copper deposits on anodized titanium implant surfaces

L. Straumann¹, A. Kessler¹, U. Pieles¹, M. de Wild¹, C. Jung²,

¹University of Applied Sciences Northwestern Switzerland, School of Life Sciences, Muttenz, CH

²KKS Ultraschall AG, Medical Surface Center, Steinen, CH

INTRODUCTION: Functionalizing implant surfaces by antibacterial copper represents a promising strategy to reduce the risk of infections immediately or years after implant placement. Besides an efficient antibacterial activity, the copper deposits should show a sufficient adhesion onto the implant surface to ensure stability under surgical handling. Here, we report results of the adhesion strength tape test according to [1] and the insertion test in analogy to [2].

METHODS: Discs (Ø14 mm) and rods (Ø4 mm, 40 mm long) of cpTi were anodized according to the spark-assisted anodizing method [3]. Copper was electrochemically deposited using proprietary electrolyte and process parameters TioCelTM), see Fig 1a. The amount of Cu was determined by EDX analysis on a unique location on the discs resp. the rods before the tape test or the insertion test (1000x magnification). On the rods, two well-defined positions, 3 mm and 15 mm from the apical end were distinguished, see Fig. 1b. In the tape test, the flaking effect of three different tapes was investigated. After a pushing period of 90 seconds, the tape was removed rapidly as close as possible parallel to the disk surface.

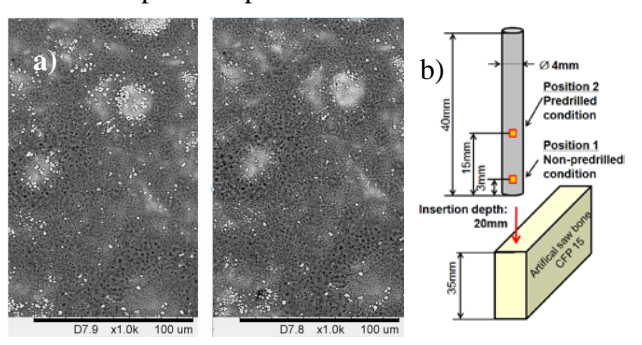


Fig. 1: a) original (left) and taped (right) surface. b) Scheme of the insertion test.

In the insertion test, the rods were pushed into a piece of polyurethane saw bone type CFP 15 [4] with the help of a guide. Subsequently, the artificial bone was cleaved to remove the treated rod. The lower position simulates an insertion into the pristine bone whereas the upper position resembles the implant placement into a predrilled hole. After the mechanical tape or insertion tests, a second EDX measurement was done on the identical surface area to determine the amount of Cu on the individual disc or rod.

RESULTS: In the tape test, the mean loss of copper was 13.0±7.7% for three different tapes, each tested on three different samples (see Fig. 2).

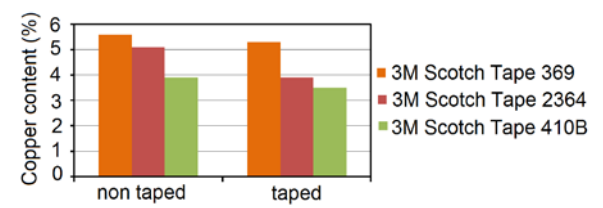


Fig. 2: Amount of copper (determined by EDX considering 5 elements) on discs before (non-taped) and after (taped) the adhesion tape test.

In the insertion tests, higher wear rates were observed at the front position rod (non-predrilled) which caused the Cu amount to be reduced by ~ 24.2% (Fig. 3a). In contrast, the predrilled, upper location simulates an insertion of an implant into a prepared hole with lower shear forces. In our experiment, the Cu amount was not significantly reduced at these locations (~ 1.7%) of the rods.

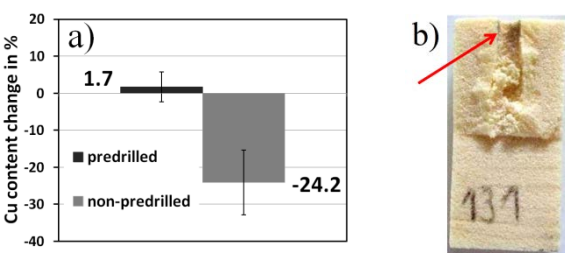


Fig. 3: a) Change in copper concentration on different rods (n=6) after the insertion test in saw bone. b) Residual Cu was detected at the saw bone counterpart.

DISCUSSION & **CONCLUSIONS:** The maximal loss of Cu from the anodized and Cu functionalized titanium surface after adhesion tape test or insertion test is in a range of $\sim 24\%$ which is regarded to be acceptable for application purposes.

REFERENCES: ¹ASTM D3359-02, Standard Test Methods for Measuring Adhesion by Tape Test. ²ASTM F 543-07, Standard Specification and Test Methods for Metallic Medical Bone Screws. ³C. Jung (2010) European Cells and Materials, **19** (Suppl. 2):4. ⁴ASTM F 1839-08, Standard Specification for Rigid Polyurethane Foam for Use as a Standard Material for Comparative Testing Orthopedic Devices and Instruments.

ACKNOWLEDGEMENT: We acknowledge funding by CTI (N°14293 2 PFNM-NM).



Entrapped biological residuals as a cause of ceramic femoral head *in vivo* failures

B Weisse¹, S Valet¹, Ch Affolter¹, M. Zimmermann²

¹Empa. Swiss Federal Laboratories for Materials Science and Technology, Laboratory for Mechanical Systems Engineering, Dübendorf, Switzerland. ²Metoxit AG, Thayngen, Switzerland.

INTRODUCTION: Today, total hip replacement using modular prostheses constitutes a state-of-theart procedure. Most of the modular prostheses consist of a titanium alloy stem, a ceramic femoral head and a titanium alloy acetabular cup, which contains a polyethylene inlay as articulation interface. Although the probability of in vivo failure of ceramic heads is very low (0.004-0.05% 1), all possible measures should be taken to decrease it further. Besides material flaws and overloading, entrapped residuals implantation can induce fractures of the ceramic head in the long term². Fragments of in vivo broken heads have been reported to exhibit asymmetric metal markings on the cone surface, which endorse the assumption that asymmetric load was applied to the head (fig. 1, left). We hypothesise that entrapped biological residuals are an important contributor to the observed asymmetric metal markings unlike asymmetric loading.

METHODS: The influence of the asymmetric physiological load configuration on resulting metal markings in the cone surface of an alumina femoral head with and without biological residuals (such as blood, soft tissue and bone chip) was investigated. Static and cyclic tests on heads were carried out in a load configuration of 0° (ISO 7206-10) and 40° (asymmetric, angle between the femoral neck axis and load direction) in a physiological environment (fig. 1, right). Image analyses of the metal marking were carried out to gain a better understanding of the processes that contribute to the generation of metal markings.

RESULTS: A decrease of the static fracture load of up to 90% was found when residuals such as bone chip, soft tissue, or blood were present. Different types and sizes/quantities of residuals in the conical surface yield strongly asymmetric metal marking patterns in a load configuration of 0° and 40° in static and cyclic tests. Without residuals in the taper fit, asymmetric loading did not result in significant differences of the metal marking compared to axisymmetric loading. All heads tested without residuals exhibited an almost

homogenous distribution of metal markings around the circumference of the ceramic cone surface at the proximal end of the bore hole.





Fig. 1, left: Explanted fractured alumina head with asymmetric residual metal markings (Metoxit AG), right: Setup with asymmetric physiological load configuration (40°) for cyclic tests (Empa).

DISCUSSION & CONCLUSIONS: Asymmetric metal markings observed on the heads tested in this investigation can be related to the presence of residuals entrapped in the taper fit. Homogenous metal mark distributions around the circumference indicate proper assembly of the head without entrapped residuals. It should, however, be noted that different taper designs may possibly result in different marking patterns. Since any alteration of the interface between metal taper and ceramic head through residuals yields a non-uniform load transfer leading to a reduction of the fracture load, an absolute clean interface is of primary importance.

REFERENCES:

¹ Tateiwa T, Clarke IC, Williams PA, Garino J, Manaka M, Shishido T, Yamamoto K, Imakiire A: Ceramic total hip arthroplasty in the United States: safety and risk issues revisited. Am J Orthop 2008, 37:E26-E31. ² Wuttke V, Witte H, Kempf K, Oberbach T, Delfosse D. Influence of various types of damage on the fracture strength of ceramic femoral heads. Biomedical Engineering 2011, 56:333-339.

ACKNOWLEDGEMENTS: This study was carried out in collaboration with Metoxit AG and was partly financed by CTI.



High-energy microtomography using synchrotron radiation at PETRA III / DESY for the 3D characterization of caries lesions

<u>Felix Beckmann</u>¹, <u>Iwona Dziadowiec</u>², <u>Lars Lottermoser</u>¹, <u>Peter Thalmann</u>², <u>Julia Herzen</u>^{1,3}, <u>Imke Greving</u>¹, <u>Georg Schulz</u>², <u>Simone E. Hieber</u>², and <u>Bert Müller</u>¹

¹ Helmholtz-Zentrum Geesthacht, Institute of Materials Research, Geesthacht, Germany

INTRODUCTION: In the present study synchrotron radiation-based microtomography was applied to characterize a human tooth with rather small, natural caries lesions and an artificially induced lesion provoked by acidic etching. The high X-ray photon statistic allows to access the detailed spatial distribution of the mineral loss induced by caries.

MATERIALS & METHODS: We perform high density resolution micro tomography using monochromatized synchrotron radiation optimized for the investigation of the spatial distribution of the mineral loss in human tooth. Since the dose for such studies is intolerable the measurement was perfomed after tooth extraction. The selected human tooth shows several natural caries lesions. The tooth was cut into two parts. One half was treated by acidic etching to induce an artifically lesion. The experiment was performed at the beamline P07 operated by HZG at the storage ring PETRA III at DESY, Hamburg, Germany. Both halves of the tooth were separately visualized from 2400 radiographs with an asymmetric rotation axis using the photon energy of 45 keV.

RESULTS: In figure 1 the demineralization caused by natural caries can clearly be seen. The 3D representation of this part of the tooth is shown in figure 2 (top). The volume rendering of the second half of the tooth treated by acidic etching is shown in figure 2 (buttom).

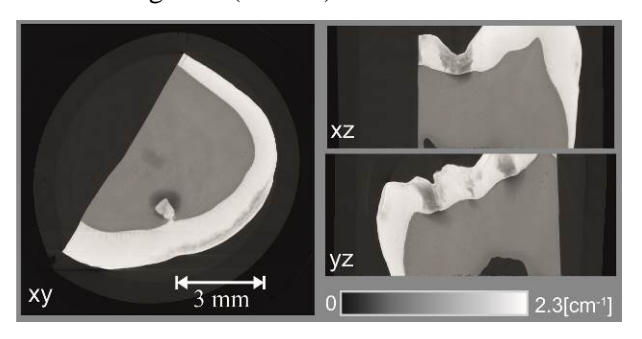


Fig. 1: Reconstructed slice (left) and vertical cuts through the reconstructed volume (right) of one

half of a human tooth after extraction showing the demineralization due to natural caries

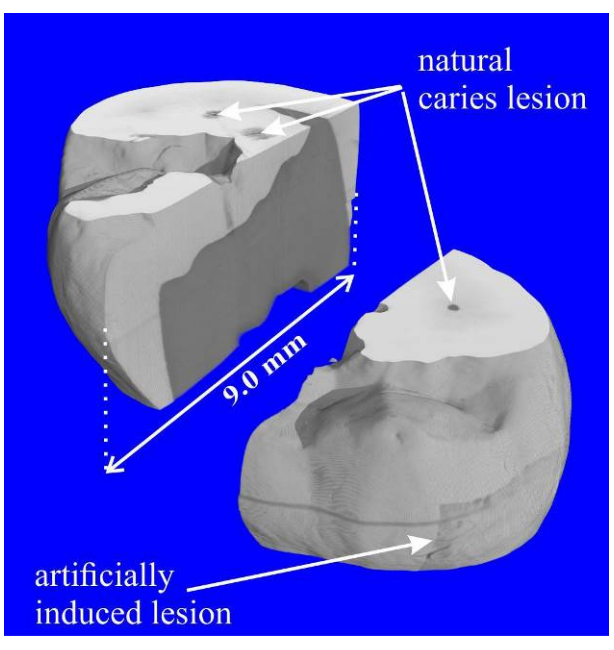


Fig. 2: Volume rendering of the two halves of the human tooth showing the location of the natural caries lesions and the artificially induced lesion.

DISCUSSION & CONCLUSIONS: The presented study allows us to compare natural and artificial lesion within the same tooth. This enables us to judge how far the man-made etching procedure corresponds to the naturally occurred caries process. Such a comparison is essential for reliable tests of remineralization strategies, as the artificial lesions can be prepared in reproducible manner for the optimization purposes.

REFERENCES: ¹H. Deyhle et al. (2014)^{*} *Nanostructure of the carious tooth enamel lesion* Acta Biomaterialia 10 (1) 355-364.

²F. Beckmann et al. (2008) *High density resolution microtomography* Proc SPIE **7078**: 70781D



² Biomaterials Science Center, University of Basel, Switzerland

³ Chair for Biomedical Physics, TU München, Garching, Germany

Osteoinduction and survival of human osteosarcoma MG-63 cells on nanoporous hydroxyapatite scaffolds

F Burgio¹, M Beaufils-Hugot¹, S Stevanovic¹, P Chavanne¹, A Rohner¹, O Braissant², P Gruner³, R Schumacher¹, U Pieles¹

¹ <u>FHNW</u>, University of Applied Sciences and Arts of Northwestern Switzerland, Muttenz CH, ² <u>LOB2</u>, Laboratory of Biomechanics & Biocalorimetry, University of Basel, Basel CH, ³ <u>Medicoat AG</u>, Mägenwil CH

INTRODUCTION: 3-D printed hydroxyapatite (HA) scaffolds with defined macro porosity have emerged as attractive biomaterials in tissue to reinforce engineering. In order compressive strength (CS) and change their properties, a combination of additives like biocompatible synthetic or natural (bio)polymers during the printing process, and extracellular matrix (ECM) generated by osteoblast-like cells, have been investigated. Osteoblasts are specialised fibroblasts that secrete and mineralise the bone matrix by regulating calcium deposition and mineralization. In our study, human a preosteoblast cell line (MG-63) was used as a model. Some preliminary experiments have been investigated in vitro to characterize the MG-63 differentiation on HA scaffolds by (a) cell proliferation, (b) matrix maturation and (c) matrix mineralisation studies.

METHODS: Scanning electron microscopy (SEM), MTT assay and Confocal Laser scanning microscopy (CLSM) were used to evaluate cell adhesion on HA scaffolds. Osteoblast differentiation was evaluated by determining alkaline phosphatase (ALP) activity at day 1, 3, 5, 14, 21. To quantify osteoblast differentiation, the mRNA expression of several osteoblast marker genes (ALP, OC, COL and Runx2) was assessed by a quantitative real-time polymerase chain reaction (qRT-PCR).

RESULTS: When 10⁵ cells per scaffold were seeded, cell number gradually increased with 7-fold higher after 14 days in comparison with day 1. After induction of ECM production with osteoblast stimulators (OS), qRT-PCR analysis showed a significant 9-fold increased for ALP expression (early differentiation marker) at day 3 in comparison with day 1. The matrix maturation was observed by SEM analysis (Fig 1) from day 5 to 21, and osteocalcin (mineralisation marker) was detected by immunofluorescence staining after 24 days.

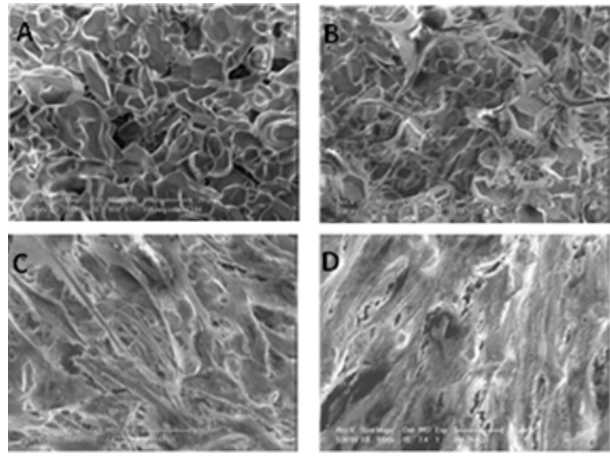


Fig. 1: SEM images of 3D-printed HA scaffolds without MG-63 cells A), and with MG-63 after 5 days B), after 14 days C), and after 21 days D) of differentiation.

DISCUSSION & CONCLUSIONS: Our preliminary studies demonstrated that MG-63 cells attached and proliferated as a monolayer over time on HA scaffolds. Our work proved also the ability of these cells to produce visible ECM after 14 days and, exhibit some mineralization indicator by the presence of osteocalcin after 24 days. Long-term mineralization studies *in vitro* will be performed with stem cells under "dynamic" conditions (Perfusion Bioreactor) to get homogeneous cell distribution and higher level of mineralization.

REFERENCES: ¹ P. Chavanne, S. Stevanovic, O. Braissant, U. Pieles, P. Gruner, R. Schumacher, (2013) 3D printed chitosan/hydroxyapatite scaffolds for potential use in regenerative medicine, *Biomed Tech (Berl)*., Issue 58. ² N. Sadr, B.E. Pippenger, A. Scherberich, D. Wendt, S. Mantero, I. Martin, A. Papadimitropoulos, (2012) *Biomaterials* **33**:5085-93.

ACKNOWLEDGEMENTS: This work is supported by a grant from the Schweizerischer Nationalfonds (SNF) (Grant number: 51NF40-144618).



Short-term delivery of fibrin-bound VEGF protein in osteogenic grafts: increased vascularization with efficient bone formation

Maximilian Burger^{1,3}, Nunzia Di Maggio², Veronica Sacchi¹, René D. Largo^{1,3}, Michael Heberer^{1,2}, Jeffrey A. Hubbell⁴, Ivan Martin², Arnaud Scherberich², Dirk J. Schaefer³, Andrea Banfi¹

¹Cell and Gene Therapy and ²Tissue Engineering, Department of Surgery, Basel University Hospital, and Department of Biomedicine, University of Basel (Switzerland)

³Plastic and Reconstructive Surgery, Basel University Hospital (Switzerland)

⁴Institute of Bioengineering, EPFL Lausanne, Switzerland

INTRODUCTION: Reconstruction of large bone defects is a major challenge in tissue engineering. Bone marrow mesenchymal stem cells (BMSC) are valuable multipotent progenitors for regenerative medicine. Spontaneous vascularization of BMSC-loaded osteogenic grafts in vivo is too slow to allow survival of the progenitors in constructs larger than a few millimeters. Stimulation of graft vascularization in vivo is needed for cell survival and efficient bone formation. Vascular endothelial growth factor (VEGF) is the master regulator of angiogenesis. However, we previously found that, while sustained over-expression of VEGF by genetically modified human BMSC was effective to improve vascularization of tissue engineered bone grafts, it also caused an undesired increase in osteoclast recruitment with excessive bone resorption [1]. Here we hypothesized that shortterm delivery of VEGF protein bound to fibrin gels may improve graft vascularization impairing bone formation.

METHODS: Primary human BMSC were retrovirally transduced to express VEGF linked to CD8, as a surface marker, or just CD8 [2]. Recombinant VEGF was engineered with a transglutaminase substrate sequence (TG-VEGF) to allow covalent cross-linking into fibrin hydrogels [3-4]. BMSC were seeded on apatite granules in fibrin pellets. Bone formation and vascularization were determined histologically 1, 4 and 8 weeks after ectopic subcutaneous implantation in nude mice.

RESULTS: One week after implantation, both the constructs with naive BMSC and fibrin-bound TG-VEGF and those with VEGF-expressing BMSC (VICD8) displayed increased vascularization compared to the controls with naive BMSC only. After 4 weeks fibrin gels were completely degraded in all conditions. After 8 weeks both fibrin-bound TG-VEGF and VEGF-expressing BMSC induced significantly increased vascularization compared to naive BMSC only (white arrows in Fig.1). However, while bone

formation was severely impaired with VEGFexpressing BMSC as expected [1], fibrin-bound recombinant TG-VEGF allowed the formation of bone tissue as efficiently as by naive BMSC alone.

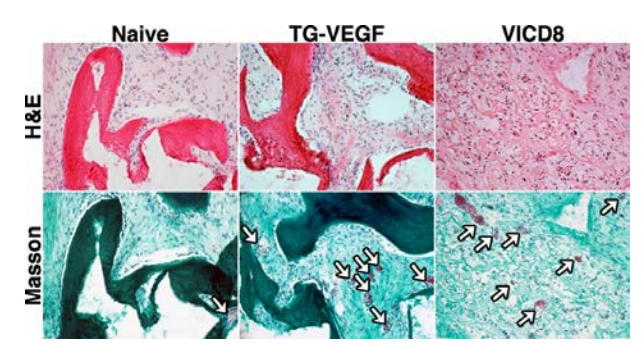


Fig. 1: In vivo bone formation by naïve BMSC, naïve BMSC with fibrin-bound TG-VEGF, or VEGF-expressing transduced BMSC, 8 weeks after subcutaneous implantation in nude mice, stained with haematoxylin and eosin (H&E) or Masson trichrome. White arrows indicate red blood cell-containing vascular structures.

DISCUSSION & CONCLUSIONS: These data suggest that VEGF effects on promoting vascularization and bone resorption can be uncoupled by short-term delivery of recombinant VEGF protein, providing an attractive and clinically applicable strategy to ensure both robust vascularization and bone formation. These data warrant further investigation in critical-size orthotopic models.

REFERENCES: ¹ U. Helmrich, N. Di Maggio, S. Gueven, et al (2013) *Biomaterials* **34**:5025-35. ²U. Helmrich, A. Marsano, L. Melly, et al (2012) *Tissue Eng. Part C* **18**:283-92. ³ J.C. Schense, J. Bloch, P. Aebischer, et al (2000) *Nat. Biotechnol.* **18**:415-9. ⁴ V. Sacchi, R. Mittermayr, J. Hartinger, et al (2014) *Proc. Natl. Acad. Sci. U.S.A.* in press.

ACKNOWLEDGEMENTS: Work was supported by an Intramural Grant of the Department of Plastic Surgery (Basel University Hospital) and by Swiss National Science Foundation grants 127426 and 143898 to A.B.



Comparing microfluidic devices and established glass capillaries in laboratorybased X-ray scattering of liposomes as nano-containers for drug delivery

M. Buscema¹, T. Pfohl², A. Zumbuehl³, and B. Müller¹

¹Biomaterials Science Center, University of Basel, Basel, Switzerland. ²Department of Chemistry, University of Basel, Basel, Switzerland. ³Department of Chemistry, University of Fribourg, Fribourg, Switzerland.

INTRODUCTION: Conventional small angle X-ray scattering (SAXS) is a powerful method to understand the morphology of self-assembled phospholipid nano-containers for targeted drug delivery. SAXS measurements are usually performed in glass capillaries. Here, we show that SAXS-signals obtained from tailored microfluidic devices, made out of a UV-curable adhesive material, poly(di-methylsiloxane) (PDMS) and polystyrene, provide additional information on the structural parameters of liposomes such as shape, size, and bilayer thickness. The flow conditions can be adjusted to study clinically relevant situations.

MATERIAL AND METHODS: We tested two phospholipids, the 1,2-diester DPPC and the 1,3diamide Pad-PC-Pad. DPPC was from Lipoid (Zug. Switzerland) while Pad-PC-Pad was synthesized as described previously.² Both lipids were hydrated with ultrapure water, submitted to freezing and thawing and then to extrusion in order to form unilamellar vesicles 100 nm in diameter³. DPPC vesicles suspensions were made at 5, 10, and 14 mg lipid per 1 ml of water and Pad-PC-Pad at 16 mg per 1 ml of water. The liposomes were tested both in glass capillaries and microfluidic devices. Glass capillaries were 1.5 mm in diameter with a wall thickness of 0.01 mm. Microfluidic devices were built using PDMS soft lithography combined with polystyrene film.⁴ The device pattern consisted of 150 and 50 µm horizontal channels. SAXS measurements were done on a Bruker Nanostar setup with a microfocus X-ray source (Cu- K_{α} -radiation, $\lambda=1.54$ Å). The beam was collimated to a diameter of about 200 µm and the signal was recorded using a 2D HiStar detector (Bruker AXS, Madison, WI, USA). Measurements in glass capillary were carried out under vacuum condition and in microfluidic devices under atmospheric pressure.

RESULTS: Figure 1 shows the *q*-plot of DPPC vesicles obtained from the glass capillary (integration time 1 hour) and from the microfluidic device (integration time 4 hours).

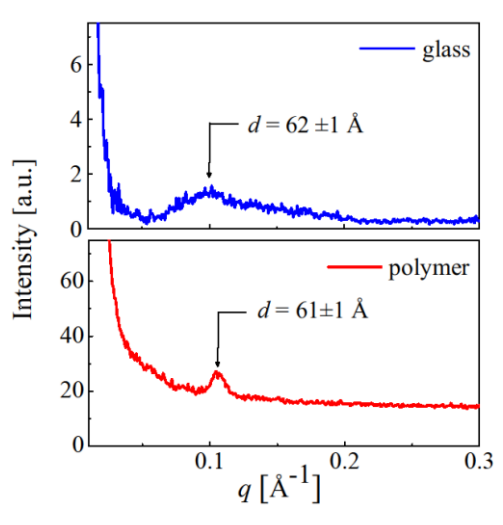


Fig. 1. SAXS signals of DPPC in glass capillary (top panel) and in a microfluidic device (lower panel) with a concentration of 14 mg/ml.

Both graphs exhibit a peak at q = 0.101 Å⁻¹ for glass capillary and q = 0.104 Å⁻¹ for microfluidic device, which corresponds to the periodicity of the lamellar structure of $d = 62\pm 1$ Å and $d = 61\pm 1$ Å respectively, characteristic for DPPC⁵. The signal-to-noise ratio is comparable for the microfluidic device and the glass capillary.

CONCLUSIONS: This SAXS-study confirms that is possible to investigate phospholipids with inhouse X-ray facility. Here, tailored polymeric microfluidic devices show comparable results with respect to the established thin-walled glass capillaries.

REFERENCES: ¹T. Saxer et al. (2013) Cardiovasc Res **99**:328-333. ²I. Fedotenko et al. (2010) *Tetrahedron Lett.* **51**:5382-84. ³P. Walde (2004) *Encyclopedia of Nanoscience and Nanotechnology* **9**:43-79 ⁴B. Weinhausen, S. Koster (2013) *Lab Chip* **13**:212-15. ⁵D.V.Soloviov et al. (2012) *J Phys: Conf Ser* **351**:012010.

ACKNOWLEDGEMENTS: This work was funded by the Swiss National Science Foundation via the national research program NRP 62 'Smart Materials'.



Bioactive DegraPol® electrospun scaffold produced by emulsion electrospinning for tendon repair application – scaffold characterization and release kinetics of biomolecules

Olivera Evrova^{1, 3}, Joanna Houska¹, Maurizio Calcagni¹, Eliana Bonavoglia², Pietro Giovanoli¹, Viola Vogel³, Johanna Buschmann¹

INTRODUCTION: Emulsion electrospinning is a technique used for production of bioactive scaffolds, offering easy incorporation of growth factors and proteins into electrospun fibers. Carrier produced by this technique system DegraPol® (DP®) as a biocompatible material can be applied in the field of tendon repair, delivering PDGF-BB at the site of injury, thus accelerating the healing process and preventing adhesion Characterization of formation. such electrospun scaffold as delivery device is necessary.

METHODS: Electrospinning parameters for production of DP® electrospun scaffolds were determined and adjusted for emulsion electrospinning. Fluorescein, FITC-BSA and BSA were chosen as model fluorophore/proteins to assess the release of biomolecules from the electrospun scaffolds. Water-in-oil emulsion was produced, using different wt % of polymer solution (8 and 10 wt %). The emulsion was produced by magnetic stirring for 2 hours or by using ultrasonication probe at 50 % power for 2 minutes. The produced emulsion was directly electrospun using in-house built electrospinning device, consisting of a programmable syringe pump, a spinning head with a blunt end made of stainless steel tube, high voltage power supply and a cylindrical collector. Different flow rates and kV were used to produce fibers with different diameters. The produced scaffolds were placed in 1xPBS (pH 7.4) and were incubated under static conditions at 37 °C and 5 % carbon dioxide. At various time points, up to 10 days, the medium was removed and the amount of the biomolecule measured (fluorescence spectroscopy (Fluorescein and FITC-BSA) or BCA protein assay (BSA)) and new medium was added. The incorporation, loading efficiency and cumulative release (%) of the biomolecules of interest were compared as a function of the fiber diameter, wt % of the polymer solution and way of emulsion preparation.

RESULTS: Increase in fiber diameter during electrospinning changes the loading of the molecule, with bigger fibers incorporating more molecule of interest. Emulsion preparation by ultrasonication probe allowed for good and quicker emulsion formation, and good distribution of the molecule within the fibers. The release of fluorescein and FITC-BSA or BSA differs drastically, with fluorescein being released in a burst manner, around 96 % within 1 - 2 days. FITC-BSA and BSA showed more sustained release, with 50 - 60 % released within 1 - 2 day and increase in release visible up to 7 days (around 90 %).

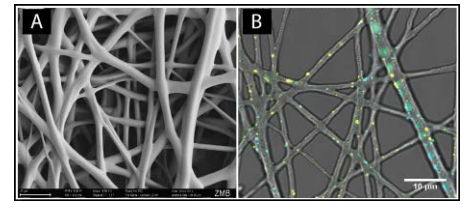


Fig. 1: Characterization of emulsion electrospun DP® scaffolds by SEM (A) and FITC-BSA loading by LSCM (B)

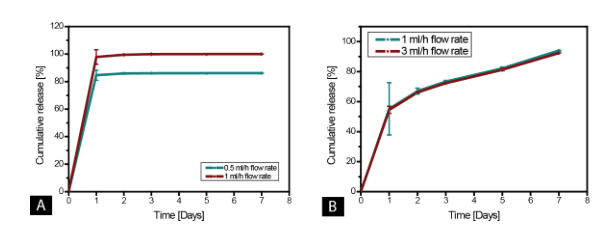


Fig. 2: Cumulative release [%] of fluorescein (A) and FITC-BSA (B) from DP® scaffolds

DISCUSSION & CONCLUSIONS: Emulsion electrospinning is an easy technique for incorporation of bioactive molecules on electrospun scaffolds and production of bioactive DP® electrospun scaffolds. These scaffolds are good carriers for different molecules of interest and the release kinetics can be tailored by the electrospinning production parameters.

ACKNOWLEDGEMENTS: This work was supported with scientific fellowship by *ab medica*, Lainate, Milan, Italy, for O.E..



¹ <u>Division of Plastic Surgery and Hand Surgery</u>, University Hospital Zurich, CH. ² <u>Ab Medica</u>, Lainate, Milan, Italy. ³ <u>Laboratory of Applied Mechanobiology</u>, ETH Zürich, CH.

Evaluation of network and pore morphology of self-assembling peptides for biomimetic therapy

F Koch¹. U Pieles¹

¹ ICB, University of Applied Sciences, FHNW, Muttenz, CH.

INTRODUCTION: Beside caries, periodontitis is nowadays a very common degenerative disease that affect adolescents and young adults. It is characterized by a microbial alteration which leads to a painful inflammation resulting in the degradation of alveolar bone, root cementum and periodontal ligament. If the progressive destruction of these three different tissues, named above, left untreated, it could lead to tooth lost. Currently, there are a lot of different treatment options like conventional invasive open flap debridement, mechanical anti-infective therapies and bone replacement grafts ¹.In the last years the idea came up to use self-repair mechanism in the patient and stimulate host's innate capacity ². This treatment strategy uses different kinds of material which were placed in a periodontal defect where progenitor/stem cells from neighbouring tissues can be recruited for in situ regeneration. In the present study newly synthesized peptides were produced to form hydrogels which could be applied through an injection in a periodontal defect without a surgery. The peptides, called P11-4 and P11-8, consist of 11 amino acids which could be triggered via pH and salt concentration to form beta-sheet structures ³. Furthermore these beta sheet structures could form higher ordered structures like fibrils and fibres leading to a 3D network that serve as extracellular matrix (ECM).

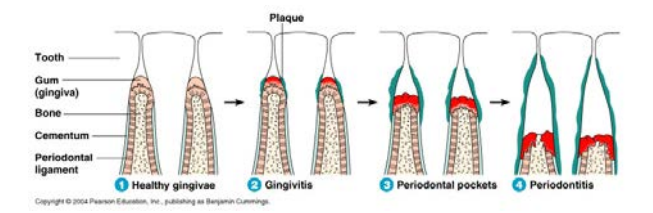
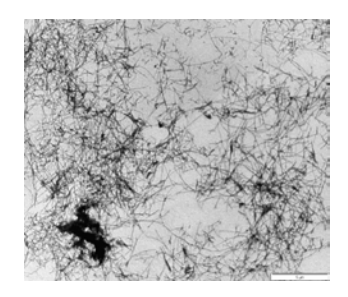


Fig. 1: The development process of periodontitis.

METHODS: The purpose of the present study was to investigate the morphology of different 3D networks and it's pore sizes and distribution under physiological conditions. Therefore TEM, SEM and tensiometry was used to estimate the potential of the nematic gels to recruit neighbouring cells in a periodontal defect.

RESULTS: The results showed first that P11-4 and P11-8 were able to form higher ordered structures like fibrils under physiological conditions which could be seen in Fig. 2a and 1b. In general it was demonstrated that the pore size ranged from 95 μm to 400 μm and their distribution of the 3D networks in an aqueous environment varied depending on used peptide concentration.



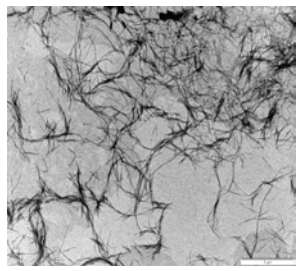


Fig. 2: TEM image of a) P11-4 (20mg/ml) and b) P11-8 (20 mg/ml) Magnification 7000 x

DISCUSSION & CONCLUSIONS: It is known from Murphy & O'Brien 2010 that ultimately scaffolds should have a balanced distribution of pore sizes between 95 µm and 325 µm. The pore size is deciding if improved cell attachment is occurring, (optimal pore size range 95 µm to 150 μm), or cell migration (optimal pore size range 300 μm to 800 μm) or also to improve diffusion of nutrients in and waste products out of the scaffold ⁴. Therefore the porous structure of self-assembled P11-4/8peptides are beneficial candidates for tissue engineering as they show an optimal pore size distribution at concentration of 20 mg/ml for in vitro experiments. The full potential of the peptides to act as a self-repair scaffold in the containment of periodontitis is still under investigation.

REFERENCES: ¹ L. Shue et al. (2012) in *Biomatter 2:4*, 271 – 277. ² F.M. Chen et al. (2010) in *Biomaterials 31 (2010) 7892* e 7927. ³ A. Aggeli et al. (2003) in *J. AM. CHEM. SOC.* 2003,125, 9619 – 96283. ⁴ C. Murphy & F.J. O`Brien (2010) in *Cell Adhesion & Migration 4:3*, 377-381



Towards contact killing antimicrobial polymer surfaces

<u>Joachim Köser¹</u>, Konstantin Siegmann², Fernanda Rossetti² and Martin Winkler²

School of Life Sciences, University of Applied Sciences and Arts Northwestern Switzerland, Muttenz, Switzerland and ²Zurich University of Applied Sciences, Winterthur, Switzerland

INTRODUCTION: Antimicrobial active surface are desirable for many medical materials. Often such surfaces are achieved either by adding active compounds to the base material or by coating processes. In both cases the antimicrobial active compounds diffuse to the surface and are slowly released over time. Here we present an alternative approach were antimicrobial active quaternary ammonium compounds (QACs) are compounded and co-extruded with polyethylene (PE) and are expected to be anchored to the surface of the final product via their hydrocarbon tails.

METHODS: QAC blended PE samples were prepared by adding 5% QACs to 95% PE granules and extrude the mixture with a twin screw Haake MiniLab Micro Rheology Compounder. The resulting samples were extracted with H₂O to release non immobilized QACs. Subsequently the samples were challenged with *S. aureus* bacteria and their antimicrobial activity analyzed by a "dead/live staining" procedure followed by fluorescence microscopy. Residual QAC release of the H₂O extracted PE samples was determined by a Kirby-Bauer type agar diffusion test.

RESULTS: The modification of polymers by surface segregating additives is well described and used routinely in the plastics industry¹. Recently PE surfaces have been modified by hydrocarbon tail terminated polyoxyethylene additives as anticalcification agents employing molecules with typical chain lengths between C_{12} and C_{18}^2 . In an analogous approach we modified PE samples by the addition of QACs with different extent of C_{18} hydrocarbon tail modifications ranging from one to four C_{18} tails. To investigate the strength of their anchoring to the polyethylene surfaces, H_2O extracted samples were employed in an agar diffusion test with *S. aureus* bacteria (Fig. 1).

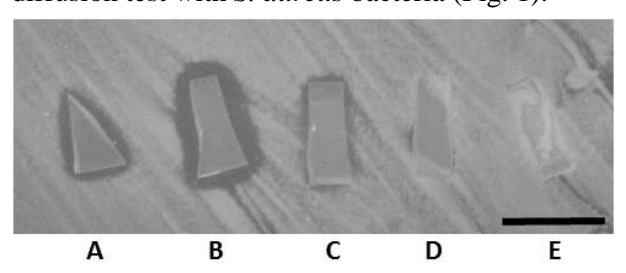


Fig. 1: Agar diffusion test of modified PE samples.



PE samples with QAC additives harbouring one (A, B), two (C), three (D) or four (E) C_{18} tails were incubated on agar plates swabbed with S. aureus. Note the growth of bacteria beneath samples D and E. The scale bar: 5 mm.

While PE samples modified with compounds A - C release antimicrobial active substances, samples D and E, corresponding to QACs with three and four C_{18} tails, do not inhibit growth of *S. aureus* in a zone around the sample.

Next the antimicrobial activity of samples D and E was examined by fluorescence microscopy of bacteria incubated on the sample surface and stained with membrane permeable ("live stain", syto 9, green) and membrane impermeable ("dead stain", propidium iodide, red) DNA stains (Fig. 2). While in most experiments the majority of bacteria died on sample D, sample E did not exhibit antimicrobial activity.

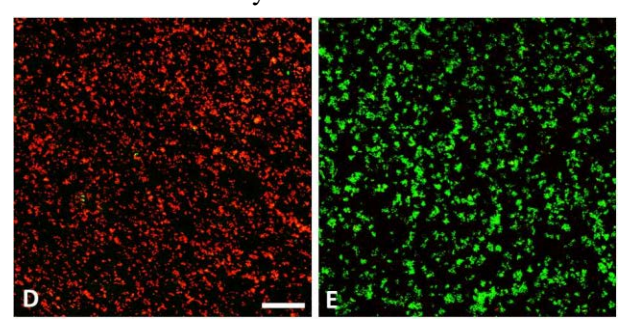


Fig. 2: Microscopical images of "dead/live stained" S. aureus following overnight incubation on PE samples D and E. Scale bar: 50 µm.

DISCUSSION & CONCLUSIONS: Here we present data on the preparation of antimicrobial active PE surfaces by surface segregation of QAC additives. Our results indicate a crucial importance of the number of QAC hydrocarbon tails for the antimicrobial activity of the modified polymers.

REFERENCES: ¹ G. Wypych, *Handbook of Antiblocking, Release, and Slip Additives*. ChemTec Pub. (2005); ² K. Siegmann, R. Sterchi, R. Widler, M. Hirayama, Lime repellent polyethylene additives. *Journal of Applied Polymer Science* (2013), 129, 2727-2734

ACKNOWLEDGEMENT: The authors acknowledge the financial support by the Swiss Commission for Technology and Innovation.

Modifications of polycaprolactone films crystallinity in terms of tissue engineering applications

D Kolbuk, P Denis, J Dulnik, P Sajkiewicz

¹ Institute of Fundamental Technological Research, Polish Academy of Sciences, Warsaw, PL

INTRODUCTION: Few research groups have highlighted the unexpected degree of cell proliferation depending on the degree of crystallinity of the substrate [1-3]. Commonly used methods of forming three-dimensional scaffolds do not take into account crystallinity optimisation. The aim of proposed presentation is to investigate polycaprolactone (PCL) substrate supermolecular structure effect, mainly crystallinity, on cells spreading, activity and proliferation.

METHODS: PCL $M_n = 10k$, $M_n = 45k$ and $M_n = 80k$ g/mol were used. As a solvents: HFIP (H) and Acetic Acid (AA) were used.

The first step of the methodology are experimental studies with a view to select process conditions to form polymeric foils with different degree of crystallinity. Two methods of foil preparation were analysed:

-forming from melt (PCL10, PCL45, PCL80) -forming from solution (e.g. PH10, PH45, PAA45) In both methods, the degree of crystallinity is modified by using different PCL molecular weight and solvents as well as annealing at different temperatures .

Degree of crystallinity was analysed using differential scanning calorimetry (DSC). Foil topography was analysed using atomic force microscopy (AFM). Selected mechanical properties and hydrophilicity (contact angle) significant from the viewpoint of cellular activity were determined. L929 cells adhesion and morphology was analysed by immunohistochemical staining for actin and nuclei at day 3. Cell activity was anlysed by MTT test.

RESULTS: Dependence of crystallinity from DSC measurements on PCL casted films from AA and HFIP solution in different concentration, using different molecular weight was analysed (Figure 1). No significant changes of crystallinity were observed for casted films PAA10 in comparison to PAA45, PAA80 in different concentration. Our modulations of solution concentration led to formation casted films with crystallinity in the range 0,51-0,68 (Fig.1). Generally, film crystallinity formed from HFIP is lower than from AA as a results of lower boiling point of HFIP. Additional annealing enables an increase of

crystallinity to 0,83. Mechanical properties strongly depends on crystallinity. Films topography changes from the flat (films from the melt) to the wavy (undulate- films from the solution) which governs the contact angle. All PCL films were found as nontoxic for L929 cells (Fig.2). Differences in cells spreading, activity and proliferation degree were found.

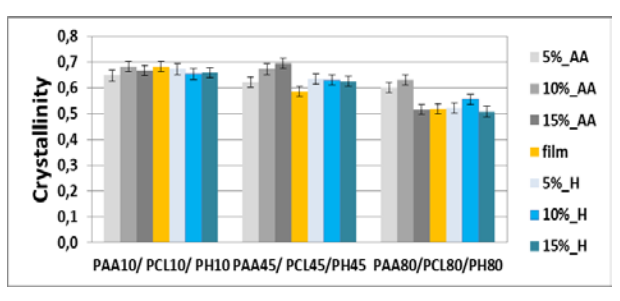


Fig. 1: Crystallinity of PH and PAA and films from the melt measured by DSC

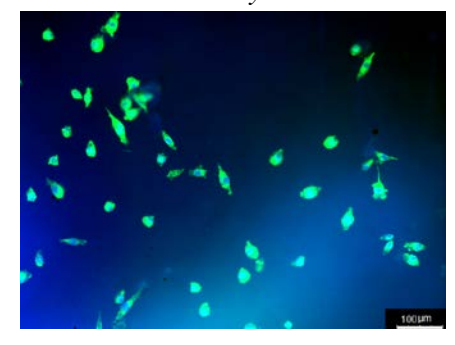


Fig. 2: L929 on PCL45

DISCUSSION&CONCLUSIONS: Modification of molecular weight, solvent and concentration of PCL enables formation of films with wide range of crystallinity. Additional annealing is an effective way of increasing crystallinity. Cells during invitro study interact with the substrate. Crystallinity as part of the supermolecular structure governs the cellular response.

REFERENCES: ¹ A. Park and L.G. Cima (1996) J Biomed Mater Res **31**:117-130. ² D. Hanein, H. Sabanay, L. Addadi and B. Geiger (1993) J Cell Sci **104** 275-288. ³ G. Balasundaram, M. Sato, T.J. Webster 2006 Biomat **27**: 2798-805

ACKNOWLEDGEMENTS: This paper has been supported by Polish National Science Centre Grant 2013/09/D/ST8/04009.



Precise tailoring of hyaluronan-tyramine hydrogels using DMTMM conjugation

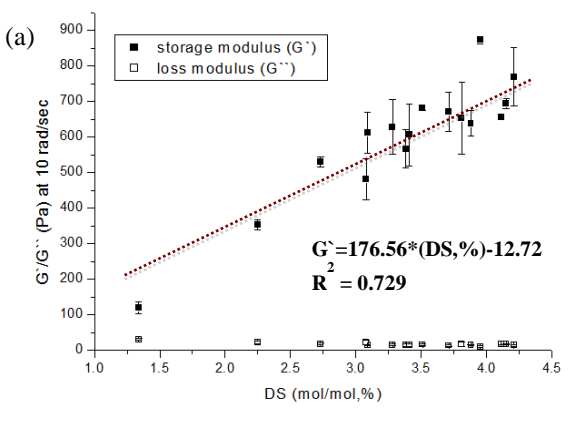
C Loebel^{1, 2}, M D'Este¹, M Alini¹, M Zenobi-Wong², D Eglin¹

¹ AO Research Institute Davos, Davos Platz, CH; ² Cartilage Engineering and Regeneration Laboratory, Department of Health, Science and Technology, ETH Zurich, CH

INTRODUCTION: Due its good biocompatibility, biodegradability and excellent gel-forming properties, tyramine-based hyaluronan hydrogels (HA-tyr) show great potential in tissue engineering and regenerative applications ^{1, 2}. Reported synthesis procedure for HA-tyr has drawbacks such as undemonstrated control over the hydrogel properties and the high tendency for formation of byproducts¹. We hypothesized that 4-(4,6-dimethoxy-1,3,5-triazin-2-yl)-4-methylmorpholinium chloride (DMTMM) is a quick and effective coupling agent for the controlled synthesis of HA-tyr conjugates and permits the precise tailoring of the hydrogel properties for cell encapsulation.

METHODS: HA-tyr conjugates were prepared by coupling tyramine to the carboxylic groups of HA at different molar ratio using DMTMM as conjugation agent. The degree of substitution (DS) was measured by UV/Vis spectrophotometry (n=3) and ¹H NMR. HA-tyr conjugates were cross-linked with HRP (1 Unit/ml) and H₂O₂ (0.34 mM) and hydrogel properties were investigated using rheology, mechanical testing, swelling and enzymatic degradation assays (n=3). For cell compatibility, human mesenchymal stromal cells (hMSCs) were encapsulated in HA-tyr hydrogels. Cell viability was assessed with Live-Dead stain and imaged with fluorescence microscopy.

RESULTS: The efficiency of DMTMM could be demonstrated by low amounts of non-functional adducts while achieving high degree of substituted tyramine on HA. We were able to achieve various DS's depending on the time and temperature during DMTMM conjugation and therefore tune the mechanical properties of the HA-tyr hydrogels with novel accuracy. At a constant HA-tyramine concentration, storage modulus (G') was varied from 100 to 900 Pa by increasing the DS (R²=0.729) while maintaining constant HRP and H₂O₂ (0.34 mM) concentrations (Fig. 1a). Interestingly different concentrations of H₂O₂, suitable for cell encapsulation, enabled additional tuning of the mechanical properties. A linear correlation could further be demonstrated for swelling (R²=0.896) and degradation properties of the cross-linked matrices. Excellent cell-compatibility of HA-tyr hydrogels supports their application as a biomaterial for cell culture (Figure 1b).



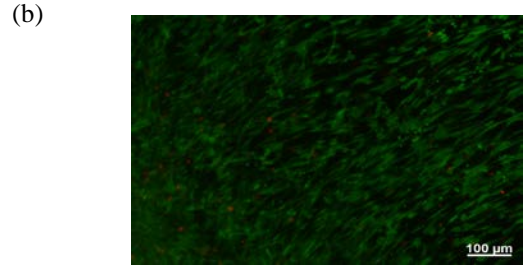


Figure 1(a) Frequency sweep of cross-linked hydrogels (2.5 % (w/v)) at 10 rad/sec in relation to the DS in mol% (n=3) with G` (filled shapes) with R^2 =0.729 and G` (empty shapes), (b) Live-Dead stain of hMSCs encapsulated in 2.5 % HA-tyr after 48h in culture.

DISCUSSION & CONCLUSIONS: DMTMM is a mild and efficient agent for HA-tyr conjugate synthesis. HA-tyr derivatives have controlled DS's allowing precise tailored hydrogel matrices that are useful for precise manipulation of microenvironment for stem cells encapsulation.

REFERENCES: ¹Darr & Calabro, 2009; Kim et al., 2011; ²Lee, Chung & Kurisawa, 2008

ACKNOWLEDGEMENTS: The authors are grateful to Mrs. D. Sutter from ETH Zurich (Switzerland) for performing NMR analysis. The authors gratefully acknowledge the financial support from the SNF and the European Science Foundation, COST Action 1005 NAMABIO.



Validation of a mechanical preparation method to isolate human adipose tissuederived cells from excision fat

N Menzi¹, R Osinga¹, A Todorov², A Scherberich², I Martin², DJ Schaefer¹

INTRODUCTION: Adipose tissue has gained popularity as a source of cells, both in a clinical and experimental setting. The cellular component gained after digestion and centrifugation of adipose tissue is typically referred to as the stromal vascular fraction (SVF). It includes various cell populations, such as fibroblastic colony-forming cells, vascular / endothelial cells and hematopoietic cells. These cells are either freshly used or seeded onto tissue culture plastic. in order to select the adherent population, known as adipose derived mesenchymal stem/stromal cells (ASC). ASC share several characteristics with bone marrow derived stromal cells (BMSC), therefore being an attractive and easily accessible source for mesenchymal stem cells (MSC) in tissue engineering.

SVF can be isolated from lipo-aspirates as well as from excision fat. The gold standard for processing excision fat is to manually mince it into 2-4mm measuring pieces in order to be digested thoroughly.

The aim of this study was to find and validate a mechanical preparation method, to optimize the mentioned time consuming procedure. Two commercially available meat grinders were therefore evaluated and compared to the gold standard.

METHODS: Excision fat from 5 different donors was processed manually with two scalpels (gold standard) and with two randomly acquired meat grinders, which withstood sterilization. SVF was gained from all three methods, following a previously described protocol for manual SVF-isolation [1]. Isolation yield, viability, clonogenicity and characterization of the SVF, as well as the differentiation potential of the resulting ASC were assessed in all three conditions.

RESULTS: Viability of all three methods did not differ significantly. Compared to the manual preparation, both meat grinders resulted in a higher isolation yield and higher clonogenicity. Multilineage differentiation showed better results

in both meat grinders. The cytofluorimetric profile of the SVF was comparable in all three conditions.

DISCUSSION & CONCLUSIONS: In this study, we validated two different specimens of meat grinders for tissue size reduction of excision fat samples for the isolation of SVF. This alternative method allows a low-cost and time-effective isolation process. In all experiments, the meat grinders performed at least as good as the current gold standard. This simplification is mainly expected to support laboratory purposes in the field of ASC tissue engineering.

REFERENCES: ¹ Güven et al. (2012) Validation of an automated procedure to isolate human adipose tissue-derived cells by using the sepax® technology. Tissue Eng Part C Methods;18(8):575-82



¹Department of Plastic, Reconstructive, Aesthetic and Hand Surgery, University Hospital of Basel

² Institute for Surgical Research and Hospital Management (ICFS), University Hospital of Basel

Nanostructured Pluronic Hydrogels for Bioprinting

Michael Müller¹, Marcy Zenobi-Wong¹

¹ Cartilage Engineering + Regeneration, ETH Zürich, Zürich, Switzerland

INTRODUCTION: An ideal bio-ink for extrusion printing should have a low initial viscosity so that it can be combined with other polymers, peptides or cells. After mixing, the flow behavior must be compatible with an extrusion printing process and. for printing fidelity, immediate cessation of flow upon deposition necessary. thermoresponsive block co-polymer poly(ethylene oxide)-poly(propylene oxide)-poly(ethylene oxide) (Pluronic) has excellent rheological properties for high resolution printing, but its cytotoxic effects at printable concentrations has deterred widespread use. 1 At lower concentrations however, cytotoxic effects are not present.² We investigated blends of acrylated and unmodified Pluronic for bioprinting applications. An initial total Pluronic concentration which is suitable for extrusion bioprinting was selected. After crosslinking of the printed construct, unmodified Pluronic is eluted out so that the final Pluronic concentration is in the range where no cytotoxic effects are present. hypothesize that this method creates nanostructured hydrogels that improve survival compared to higher concentration Pluronic gels.

METHODS: Acrylated Pluronic F127 (PF127-DA) was synthesized as described elsewhere.³ The blends of acrylated (AC) and unmodified Pluronic (PF) were analyzed with rheometry to evaluate their gelation temperatures and mechanical properties. Chondrocyte viability was assessed with a Live/Dead assay after 7 days following photoencapsulation in the PF127 hydrogel blends. 1% w/v Alginate beads were used as a control. A bioprinter (BioFactory,RegenHu, Villaz-St-Pierre, Switzerland) equipped with a solenoid valve and a needle with 300 μm diameter was used to create the hydrogel scaffolds.

RESULTS: Increasing amounts of acrylated PF127 increased the gelation temperature of the mixtures but never exceeded 37°C. The ink could be deposited with high accuracy (see Figure 1) onto heated substrates and the printed structures were mechanically stable after UV crosslinking with storage moduli between 10 and 20 kPa before the elution of the unmodified PF127. Cell viability was dramatically increased compared to gels consisting only of acrylated Pluronic (PF0AC20 - Figure 2).

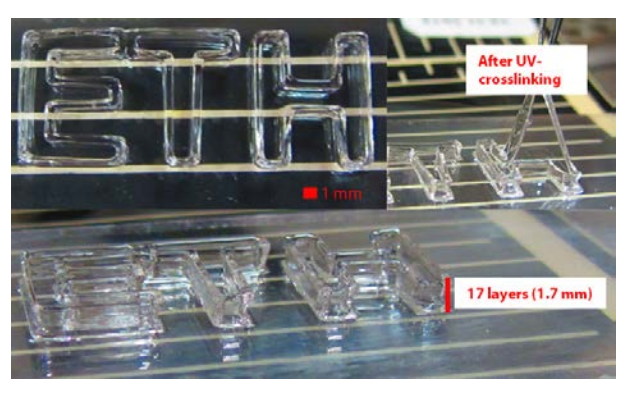


Fig. 1: Printing onto heated substrate with the PF17AC3 ink composition.

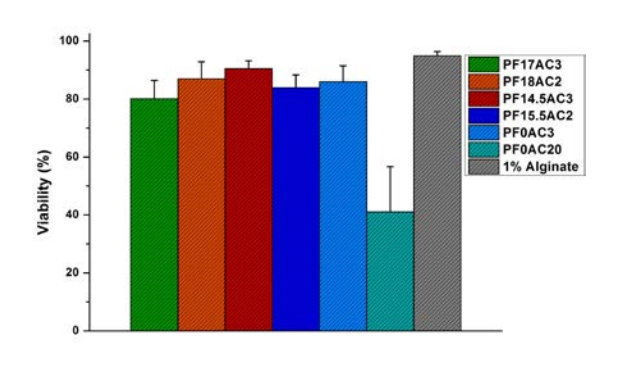


Fig. 2: Cell viability of embedded chondrocytes 7 after encapsulation in the nanostructured hydrogels.

DISCUSSION & CONCLUSIONS: Mixing of diacrylated and unmodified F127 and subsequent UV crosslinking and elution improves cell viability while maintaining the printability of the bioink. Addition of photocrosslinkable biopolymers, adhesion peptides and degradable structures could further improve viability of the hydrogel network. The viability reported here is to our knowledge the highest achieved in Pluronic hydrogels at printable concentrations (>16% w/v).

REFERENCES: ¹ N. Fedorovich et al. (2009) *Biomacro-molecules* **10**: 1689-1696 ² Khattak et al. (2005) *Tissue Engineering* **11**: 974-983. ³A. Sosnik et al. (2003) *J. Biomater. Sci. Polymer. Edn* **14**: 227-239

ACKNOWLEDGEMENTS: The work was funded European Union Seventh Framework Programme (FP7/2007-2013) under grant agreement n⁰NMP4-SL-2009-229292.



Role of biphasic calcium phosphates in the osteonecrosis of the jaw associated with bisphosphonates

S Paulo^{1,2}, A Abrantes^{1,3}, M Laranjo^{1,3}, J Casalta-Lopes¹, K Santos^{1,3}, A Serra⁴, M Botelho^{1,3}, M Ferreira^{1,2}

Biophysics Unit, IBILI, Faculty of Medicine, University of Coimbra (FMUC), Portugal.
 Department of Dentistry, FMUC, Portugal.
 CIMAGO, FMUC, Portugal.
 Coimbra, Portugal.

INTRODUCTION: Bisphosphonate (BP-ONJ) related osteonecrosis of the jaw has been reported in patients receiving intravenous BPs, particularly zoledronic acid (ZA), with no treatment at present. ZA is used in the management of metastatic bone disease and the prevention of treatment-induced bone loss. BP-ONJ is most commonly observed following dental surgeries. BPs release from oral bone may impede the growth and migratory capacity of oral fibroblasts, inhibiting matrix deposition and remodelling of oral soft tissues, a critical aspect of wound healing ¹. On the other hand, the affinity of BPs for hydroxyapatite (HA) is used in calcium phosphate systems for controlled release of BPs, due to their antiresorptive properties. BPs-HA composites could be locally administered as a drug delivery system. Based on that affinity, it was studied the decrease of local toxicity of BPs, inherent to BP-ONJ, through the application of Biphasic calcium phosphates (BCPs - 25% b-TCP/ 75%HA) in the oral wound.

METHODS: The in vitro adsorption experiments were carried out using aqueous samples of ZA in a concentration range of 0.1 to 1 mM. To ZA solution 0.02 g of BCPs was added and the mixture was stirred at room temperature. The amount of ZA absorbed by BCP was known by measuring the ZA absorbance with time comparing with the initial ZA absorbance. Discarded gingival surgical tissue was collected from ten donors after informed consent was obtained (Ethics Committee of FMUC) for primary human oral fibroblasts culture establishment. A solution of ZA was incubated with stirring during 3 days in the absence and in the presence of BCP. Cells were exposed to clinically relevant doses of these solutions (5, 25, 50 and 100 μM), according to ISO Standards 10993-5 for cytotoxicity testing. The metabolic activity was assessed with MTT assay at 48, 72, 96 and 120 hours. Cell viability and death pathways were evaluated by flow cytometry through double labeling with propidium iodide

(PI) and Annexin V. MTT results were fitted to dose-response sigmoidal curves. Statistical comparison between compounds for each concentration and each incubation period was performed using Student's t-test or Mann-Whitney test. Significance was established at p<0.05.

RESULTS: Capture of ZA by BCP was evident from the observed decrease in the initial absorbance value. Cell metabolism studies showed that ZA alone decreases cell metabolic activity at 96 and 120 hour, with the IC50 values of 38.13µM 38.48µM respectively. For all other conditions, we were not able to determine IC50. However, for the same conditions cells incubated with ZA-BCP are not affected by the treatment in accordance with previous studies ^{1,2}. Comparing MTT assay results between ZA and ZA-BCP for a concentration of 100µM, there were statistically significant differences for all incubation periods (p<=0.001). Considering all the other assessed concentrations there were differences between both compounds for 96h and 120h of incubation (p<0.05). The preliminary results of flow citometry studies showed no reduction of cell viability at 72 and 96 hours.

DISCUSSION & CONCLUSIONS: BCP addition to ZA solution demonstrates cell toxicity reduction by allowing metabolic recovery. It is possible that BCP might prevent changes in the oral cells, responsible for mucosal dehiscence and BP-ONJ lesions. This biomaterial seems to have wound healing properties and might be a solution for BP-ONJ.

REFERENCES: ¹ S Otto, C Pautke, C Opelz, et al. (2010) Osteonecrosis of the jaw: effect of bisphosphonate type, local concentration, and acidic milieu on the pathomechanism. *J Oral Maxillofac Surg* 68(11): 2837-45. ² M Cozin, BM Pinker, K Solemani K, et al (2011) Novel therapy to reverse the cellular effects of bisphosphonates on primary human oral fibroblasts. *J Oral Maxillofac Surg* 69(10): 2564-78. ³ E Boanini, P Torricelli, M Gazzano et al (2012) The effect of zoledronate-hydroxyapatite nanocomposites on osteoclasts and osteoblast-like cells in vitro. *Biomaterials* 33(2): 722-30.



Is Aquaporin-9 playing a role in osteoporosis?

D Petta¹, U Eberli¹, G Calamita², P Gena², V Stadelmann¹, D Eglin¹, M D'Este¹, M Alini¹

AO Research Institute, AO Foundation, Davos, CH. ² Dept Biosciences, Biotechnologies and Biopharmaceutics, University of Bari 'Aldo Moro', Bari, IT

dalila.petta@aofoundation.org

INTRODUCTION: Aquaporins (AQPs) are a family of channel proteins allowing transport of water and small neutral solutes across biological membranes. AOPs are expressed in many tissues where they play roles in fluid balance, metabolic homeostasis, and several other processes [1]. AQP9, an AQP belonging to the subgroup of aquaglyceroporins, is expressed in osteoclastlineage cells where it is suggested to be relevant to osteoclast differentiation leading to the formation large multinucleated osteoclasts consequence of a rapid influx of water and increase in cell volume. A study in mice revealed that although the AQP9 expression rises during osteoclast biogenesis, its absence does not affect the differentiation or functional activity of osteoclasts in physiological conditions [2]. A role for AOP9 in the development of microgravityinduced bone loss has also been suggested by Bu et al. [3]. While preliminary, these evidences support a potential role of AQP9 in bone resorption. In the present work, old AQP9-null mice were used to study the effect of AQP9 on bone structure.

METHODS: Adult C57BL/6 mice wild-type (WT; n = 9) and AQP9-null (knockout, KO; n = 7) 45-weeks-old were used in the study. This age is very close to the average lifespan of these mice. Whole animals were scanned by means of micro Computed Tomography (vivaCT40, Scanco Medical). Afterwards the bone mineral density (BMD), the bone fraction (BV/TV), the cortical thickness (ct.th) and the dimensions of femurs and of the 8^{th} tail vertebra were evaluated.

RESULTS: No difference in femur length between WT and AQP9 KO mice was observed Quantitative analysis of BMD and BV/TV ratio performed on the femurs didn't show significant differences. We looked further into the structures of the cortical area of the bones, finding no structural changes as well. Although not statistically significant, vertebrae in KO mice displayed higher BV/TV, BMD and ct.th.

DISCUSSION & CONCLUSIONS: Lack of AQP9 seems not to influence femur bone structure

in mice. On the contrary, vertebrae from KO mice display higher BV/TV, BMD and ct.th than WT mice. These differences were not statistically significant, possibly due to the small sample size compared to the intrinsic variability of the parameters measured. Altogether, these results are consistent with previous reports indicating decreased BMD associated with increased AQP9 expression in microgravity-induced bone loss [3]. AQP9 may reveal a new target for modulating bone loss and osteoclast activity.

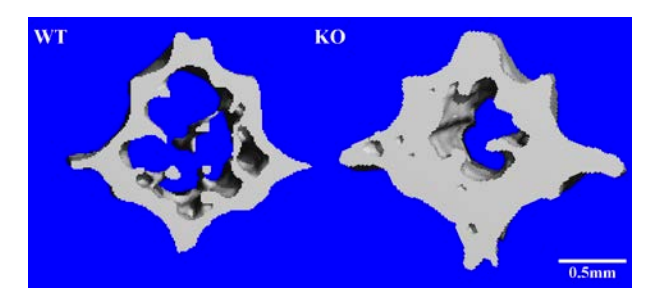


Fig. 1: 3D renderings of 40-slices thick segmented microCT sections showing the difference in vertebra cortical thickness between WT and KO. The image represents the extremes.

	Vertebra		Femur	
	WT	ко	WT	ко
BV/TV	0.65 ±0.04	0.70 ±0.05	0.46 ±0.03	0.45 ±0.02
BMD [mg HA/cm]	673 ±60	768 ±67	551 ±46	534 ±36
ct.th [mm]	0.24 ±0.02	0.29 ±0.04	0.21 ±0.02	0.20 ±0.01

Table 1. Analyses of bone structure from mice.

REFERENCES: ¹ P. Gena et al (2011), Aquaporin membrane channels: biophysics, classification, functions, and possible biotechnological applications, Food Biophysics 6:241-249 ² Y. Liu et al (2009) Osteoclast differentiation and function in aquaglyceroprotein AQP9-null mice, Biol. Cell. 101, 133-140. ³ G. Bu (2012), AQP9: A novel target for bone loss induced by microgravity, BRRC 419,774-778.



Engineering niches for intervertebral disc cells using random and aligned silk nano fibres

T Studer^{1,2}, P Fortunato², N Gadhari¹, D Frauchiger¹, R Rossi¹, B Gantenbein-Ritter^{1,2}

¹ <u>Tissue and Organ Mechanobiology</u>, Institute for Surgical Technology & Biomechanics, University of Bern, Switzerland, ²<u>Laboratory for Protection and Physiology</u>, Swiss Federal Laboratories for Material Science and Technology, St. Gallen, Switzerland

INTRODUCTION: Low back pain linked to intervertebral disc (IVD) degeneration is a highly abundant problem in the aging modern society. Until today there is no biological solution available based on the patient's autologous cells to restore or repair the IVD. We hypothesized that electrospun silk scaffolds can mimic the extracellular matrix of the IVD cells: i) a random orientation of the fibres would be ideal for nucleus pulposus cells (NPC) and ii) an alignment of the fibres would be favourable for annulus fibrosus cells (AFC).

METHODS: Silk liquefaction: Silk fibres from Bombyx mori (SwissSilk) were cut in small pieces and boiled in 0.2M Na₂CO₃ for 30 min to remove the sericine. Then, the silk fibres were rinsed three times in ultrapure water (UPW) and dried overnight. The dry silk was then dissolved in 9.3 M LiBr solution and dialysed against UPW for 48 h and purified by high speed centrifugation.¹ Electrospinning: Silk was mixed with 5% (wt/vol) 900kDa-PEO to generate a solution of 6.4% silk and 1 % (wt/vol) PEO. This solution was electrospun on a flat collector for randomly oriented fibres and on a rotating mandrel for aligned fibres. Of each electrospun mat N=40 samples of 6mm diameter were punched out. N=20 of the randomly aligned samples were ultrasonicated for 1 min at 80 Watts to increase their porosity.² Cyto-compatibility: 40k human derived NPC and AFC (ethically approved) were seeded per carrier and grown for 7 days. On day 1 and 7 cell spreading (cLSM) and cell activity (Alamar Blue) and DNA content was monitored.

RESULTS: The electro-spinning process revealed two completely different scaffold and micro environments for cells as confirmed by SEM (Fig. 1, A,B) Live/dead stain of IVD cells confirmed their alignment in the direction of the parallel-oriented fibres (Fig. 1, C, D). On day 7 cell activity decreased for AFC to the contrary for NPC were it increased per cell (Fig. 2) Generally, it was noted that cells adhered and proliferated better on ultra-sonicated non-oriented scaffolds than on aligned scaffolds (data not shown).

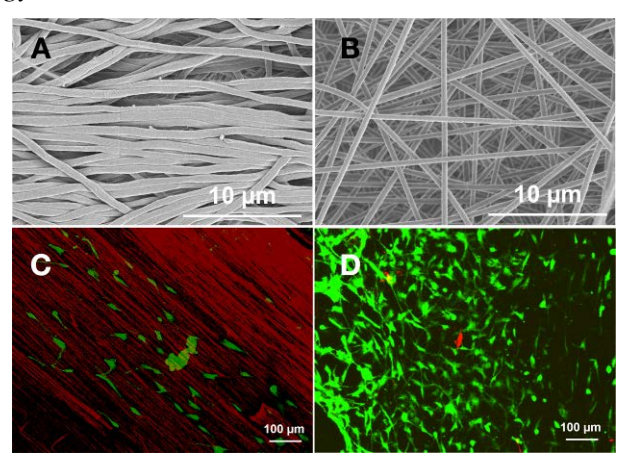


Fig 1: A-B) Scanning electron microscopy images of scaffolds A) Aligned silk fibres (mandrel speed=30Hz) B) Randomly distributed silk fibres C-D) Human IVD cells on scaffolds C) AFC aligned in the direction of silk fibres (red) D) NPC randomly oriented in ramdomly aligned silk nano fibres.

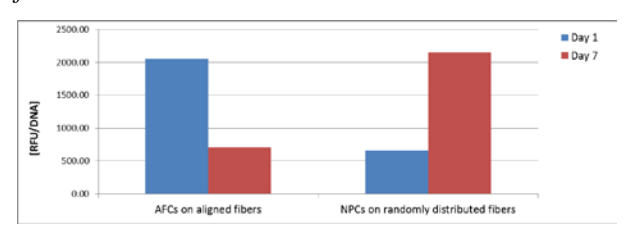


Fig. 2: Cell activity of human NPC and AFC measured with Alamar Blue Assay on day 1 and 7.

DISCUSSION & **CONCLUSIONS:** By modification of the silk composition and the electro-spinning parameters the 3D environment of a scaffold can be controlled. This is crucial for cell adhesion and proliferation of primary cells. The general direction of cell growth can be controlled by the arrangement of the silk nano fibres. Future research will focus on the control of porosity and integration of adhesion molecules and cytokines to tailor the IVD cell specific niche.

ACKNOWLEDGMENTS: This research was financed by the Gebert-Rüf Foundation project # GRS-X028/13. LM Benneker provided the IVD specimen from Trauma Spinal Surgery.

REFERENCES:

¹D N Rockwood (2011) *Nat. Protoc* **6**:1612-31. ²J B Lee (2011) *Tissue Engineering* **17**:2695-2702.



AFM nanoindentations of hydrogel scaffolds coated with hyaluronic acid for regenerative medicine

R Suriano, C Credi, C De Marco, M Levi, S Turri

<u>Dept. of Chemistry, Materials and Chemical Engineering "Giulio Natta"</u>, Politecnico di Milano, P.zza Leonardo da Vinci, 32 20133 Milan, Italy

INTRODUCTION: Stem cell fate is known to be influenced by various physical parameters properly provided in the stem cell microenvironment. Among these parameters, hydrogel substrate stiffness has been emerged as a significant signal in directing mesenchymal stem cells (MSCs) differentiation to specific lineages. In addition to stiffness, structural and geometrical features of stem cell niches have been shown to influence the MSCs functions [1]. The implementation of atomic force microscopy (AFM) indentations to characterize mechanical properties of 3D micronsized architectures is therefore an important factor understand how to direct the differentiation. In this work, AFM indentations of 3D scaffolds designed for tissue engineering were pursued and achieved. These scaffolds were coated with hyaluronic acid (HA) hydrogels crosslinked with divinyl sulfone (DVS).

METHODS: Two-photon polymerization (2PP) was used to fabricate scaffolds with a 3D spatial architecture, made of a hybrid organic-inorganic material (SZ2080), as explained in a previous work [2]. The scaffolds were dip-coated with a crosslinked HA hydrogel using a HA:DVS molar ratio of 1:10 [3]. AFM nanoindentations were performed with NSCRIPTORTM system (Nanoink) $(T = 23 \, ^{\circ}C, \text{ relative humidity} = 50\%)$. For all AFM measurements, a colloidal probe (HYDRA6R-200NG-COLL, AppNano) with a nominal spring constant $k_c = 0.035$ N/m and a spherical tip, made of SiO_2 (radius = 2.5 µm), was employed after a hydrophobic vapour phase silanization 1H,1H,2H,2H-perfluorodecyltriethoxysilane (100)°C overnight in a sealed vial).

RESULTS: Figure 1 shows force vs. indentation curves obtained by AFM on a 3D HA-coated scaffold. Taking into account that the max applied force on scaffolds was 6.7 nN, a high adhesion force of 22.4 nN was measured. To determine the elastic modulus from indentation experiments, the JKR model was used due to large adhesion phenomena observed [4]. A perfectly elastic behavior was exhibited by the indented sample, as indicated by the overlapping of the loading and

unloading curves in Figure 1. By employing the JKR equations [4], an elastic modulus of 21.5 ± 4.3 kPa was calculated, in good agreement with the values previously obtained from rheological measurements [3].

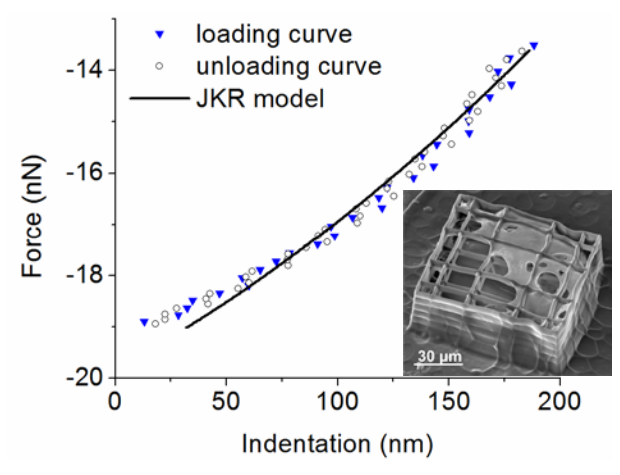


Fig. 1: Force vs. indentation curves on a 3D scaffold obtained from loading and unloading phases in the data range selected for the fitting performed by employing the JKR model; (inset) SEM image of a 3D hydrogel coated scaffold.

DISCUSSION & CONCLUSIONS: AFM nanoindentations on 3D scaffolds coated with a crosslinked HA hydrogel were successfully performed. These AFM indentations were obtained by means of a high precision x-y axis stage, carefully considering the periodic porosity of the scaffolds ranging from 10 to 30 μm and selecting a max indentation depth of 200 nm.

REFERENCES: ¹ O.Z. Fisher, A. Khademhosseini, R. Langer, et al (2009) *Acc. Chem. Res.* **43**:419-28. ² M.T. Raimondi, S.M. Eaton, M. Laganà, et al (2013) *Acta Biomater* **9**:4579-84. ³ C. Credi, S. Biella, C. De Marco, et al (2014) *J Mech Behav Biomed Mater* **29**:309-316. ⁴ H.-J. Butt, B. Cappella, M. Kappl (2005) *Surf Sci Rep* **59**:1-152.

ACKNOWLEDGEMENTS: The research was funded by Cariplo Foundation, Milano, project title "3D Micro structuring and Functionalization of Polymeric Materials for Scaffolds in Regenerative Medicine".



Near zero wear of diamond like carbon coated implants for up to 100 years of articulation

Kerstin Thorwarth¹, Dominik Jaeger¹, Renato Figi¹, Michael Stiefel¹, Bernhard Weisse¹, Ulrich Müller¹, Götz Thorwarth², Roland Hauert¹,

¹ Empa, Swiss Federal Laboratories for Materials Science and Technology, Überlandstrasse 129, CH-8600 Dübendorf, Switzerland,

² DePuy Synthes GmbH, Überlandstrasse 129, CH-8600 Dübendorf, Switzerland

INTRODUCTION: Diamond like carbon (DLC) coatings have been proven to be an excellent choice for wear reduction in many technical applications. However, for successful adaption to the MedTech field, layer performance, stability and adhesion in physiologically relevant setups are crucial and not consistently investigated. In vitro wear testing as well as adequate corrosion tests of interfaces and interlayers are of great importance to verify the long term stability of DLC coated load bearing implants in the human body [1].

METHODS: Diamond like carbon coatings were deposited on CoCrMo biomedical implant alloy (lumbar spinal disc) using a plasma-activated chemical vapor deposition (PACVD) process. As an adhesion promoting interlayer tantalum films were deposited using magnetron sputtering. The contamination level during the deposition was monitored using a QMS.

Wear tests of coated and uncoated implants were performed in physiological solution up to a maximum of 101 million articulation cycles with an amplitude of $\pm 2^{\circ}$ and $-3/+6^{\circ}$ in successive intervals at a preload of 1200 N. Within this time these implants were characterized by high wear resistance, low friction coefficients, high corrosion resistance and low defect growth. These results were obtained by means of optical microscopy, SEM/EDX, FIB cross section and profilometry. The wear fluid was analyzed using ICP OES.

RESULTS: Metal-on-metal (MoM) pairs perform well up to 5 million loading cycles, afterwards they start to generate wear volumes in excess of 20 times those of DLC-coated implants [2]. This is attributed to a slight roughening observed on unprotected metal surfaces; which is usually also observed in-vivo. The DLC on DLC inlay pairs show comparable low volume losses throughout the full testing cycle (up to 101 million cycles over a period of three years and two months).

DISCUSSION & CONCLUSIONS: After 101Mio cycles no wear of the DLC layer could be observed. Only local defects appeared within the first thousands of cycles; no defect growth was observed afterwards. No corrosive attack of the interlayer was found.

DLC combined with a Ta interlayer figured out to be an excellent wear resistive coating for joint replacements with a high lifetime (100Mio cylces of articulation in a spine simulator corresponds to 100 years of articulation in the human body).

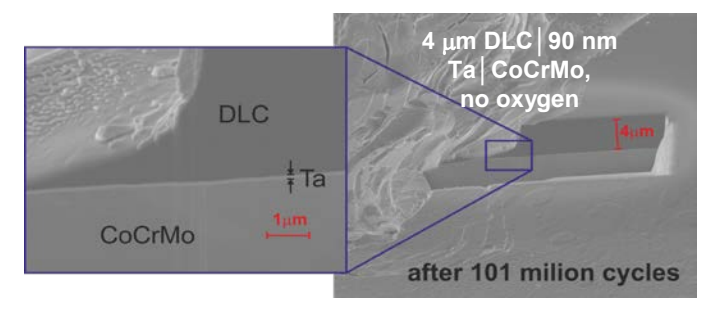


Fig. 1: Cross-section of a 4 µm thick DLC layer on a CoCrMo implant after 101 million cycles in a spinal disk simulator; the thickness comply with the original thickness of 4µm; no corrosive attack of the interlayer is observed.

REFERENCES:

- [1] R. Hauert, K. Thorwarth et al. Surf Coat Technol, **233** (2013) 119.
- [2] G. Thorwarth, C.V. Falub, U. Mueller, B. Weisse, C. Voisard, M. Tobler, R. Hauert, Acta Biomaterialia, **6** (2010) 2335.

ACKNOWLEDGEMENTS: Financial support provided by the Swiss innovation promotion agency CTI, and CCMX is gratefully acknowledged.



β-TCP platelets with high aspect ratio produced in a tubular reactor

<u>J Thüring</u>^{1,2}, L Galea¹, M Bohner¹

¹RMS Foundation, Bettlach, CH. ²ETH Zürich, Department of Materials, Zürich, CH.

INTRODUCTION: Composites verv promising bone substitute materials for load bearing sites because they can potentially combine high tensile strength and toughness. The tensile strength is strongly influenced by parameters like architecture of the composite, geometry and composition of the ceramic platelets and type of organic matrix. The ideal platelet geometry can be calculated theoretically (e.g. for β-TCP platelets embedded in a chitosan matrix: aspect ratio ≈ 28 and thickness < 350nm). But to date, these theoretical calculations have not been confirmed experimentally. Also, the largest aspect ratio ever reported for β -TCP is close to 15¹. Therefore, the aim of the present study is to produce β -TCP platelets with aspect ratios as close or even superior to 28.

METHODS: Since Galea et al² showed recently that the aspect ratio can be controlled by a change of pH, a systematic study was performed here by varying the NaOH amount. Most experiments were performed in a tubular reactor. For that purpose, a CaCl₂-ethylene glycol solution and a H₃PO₄-NaOH-ethylene glycol solution were pumped through separate tubes and heated to 90°C. After mixing in a static mixer the growth reaction occurred at constant temperature at 150°C. For comparison, a few experiments were also carried out in a batch reactor as described in the work of Galea et al.² The geometry and composition of the resulting particles were analysed by SEM and XRD, respectively.

RESULTS: Varying the NaOH concentration between 15 and 32 mmol/l in the tubular reactor led to β-TCP platelets with and aspect ratio between 4 and 50 (Fig.~I). The size dispersion of the diameter was between 0.1-0.3. But the resulting material was not pure because other phases like DCPA, HA and Cl-HA were present in the β-TCP samples. The XRD results showed that the amount of the undesired phases decreased with increasing NaOH concentration. At c_{NaOH} =22.3mM the experiment led to β-TCP platelets with and aspect ratio of about 33 and a size dispersion of the diameter of 0.2. The sample was composed of 82% β-TCP, 17% DCPA and 1% other phases. On the other hand an equal experiment performed in the

batch reactor led to β -TCP platelets with and aspect ratio of about 21 and a size dispersion of the diameter of 0.10. The sample was composed of 19% β -TCP, 81% DCPA.

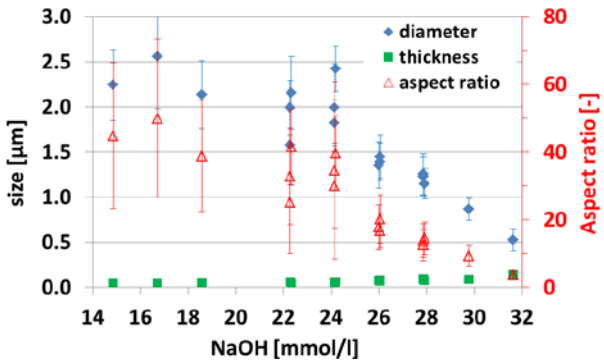


Fig. 1: Influence of NaOH on the size of the β -TCP platelets produced in a tubular reactor.

DISCUSSION & CONCLUSIONS: The results show that a change of reactor (or mixing conditions) led to a change of composition, aspect ratio, and size dispersion. The change of composition at the end of the reaction is puzzling because the initial composition was identical. To account for this change of solid composition, the pH of the solution in which calcium phosphates precipitated must have differed. Specifically, since β-TCP is more basic than DCP, the solution in the tubular reactor must have been more acidic at the end of the reaction than in the batch reactor. Interestingly, β -TCP platelets present a higher aspect ratio and size dispersion in more acidic conditions², which fits with the present data. The main question is why different mixing conditions (tubular or batch reactor) lead to different compositions. To answer this question, additional experiments will be performed with the aim to better characterize the sequence of calcium phosphate precipitation and the precipitation conditions (e.g. pH).

This work showed that very high aspect ratios can be obtained (s<50) by minimizing the NaOH amount in the tubular reactor. Also, a comparison of the two different production methods indicates that the β -TCP platelets, resulting from the tubular reactor, have a higher aspect ratio and size dispersion. Interesting, but still unclear, is the fact that both methods result in different compositions.

REFERENCES: ¹L. Galea et al (2014) *Acta Biomaterialia (in press)*. ²L. Galea et al (2013) *Biomaterials*, **38**:6388-6401. ³J. Tao et al (2008) *Crystal Growth & Design*, **8**(7):2227.



Influence of the shape of glass beads on the injection properties of β -tricalcium phosphate – glass beads – water pastes

N van Garderen¹, P Michel¹, M Bohner¹

¹RMS Foundation, Bischmattstr.12, PO Box, 2544 Bettlach, Switzerland

INTRODUCTION: Calcium phosphate cements and pastes are of great interest in non-invasive surgeries. However, when they contain granules, their rheological and injection properties are poor. Recently, our group tried to get a better understanding of this phenomenon by looking at the injectability of model pastes composed of β -tricalcium phosphate powder (β -TCP), water and spherical glass beads (100-400 μ m) [1]. Since most granular bone graft substitutes are not spherical but angular, this study aimed at determining the influence of glass beads hape on the injectability of β -TCP – glass beads – water pastes.

METHODS: β-TCP powder from Sigma-Aldrich (No 2128, Steinheim, Germany) with a density of 3.1 g.cm⁻³ and a d_{50} of 1.8 \pm 0.4 μ m was mixed with demineralized water to form a paste with a liquid-to-solid ratio of 0.45 ml/g. Spherical (Spheriglass CP01 ref. 2024 and 1619, Potters Europe) and angular glass beads (ref. ST-145 and ST-60, Reidt GmbH & Co. KG, Stolberg, Germany) with a density of 2.5 g.cm⁻³ were used. CP01_2024 (called "SS", as "small" "spherical") and ST-145 ("SA", as "small" and "angular") had a size between 106 and 212 µm, whereas CP01_1619 ("LS", as "large" "spherical") and ST-60 ("LA", as "large" and "angular") had a size between 250 and 425 µm. Pastes were homogenised one minute on a vortex and filled in a 1 ml syringe (BD Luerlock, Beckton Dickinson, USA; inner diameter: 4.5 mm, opening diameter: 1.9 mm). The plunger was then inserted so that its lowest part reached the 1 ml graduation. The syringe was placed in a metallic cylinder to avoid deformation during pressing. Injection tests were performed with a Zwicki-Line Z5.0 (Zwick, Kennesaw, GA, USA) compression tests machine. Displacement rate was fixed at 0.4 mm/s and tests were automatically stopped when a 250 N load was reached. Injectability was defined as the weight percentage of extruded material. Median beads size was determined from microscopies and sphericity was calculated from the inscribed $(d_{50 \text{ ins}})$ and circumscribed $(d_{50 \text{ circ}})$ maximum diameters.

RESULTS: Fig.1 shows that about 80% of the pastes could be injected at low bead content. As observed in our previous study, the addition of a small bead volume fraction increased significantly the injectability. However, beyond a certain volume fraction, which was higher for smaller and spherical beads (20 vol.% for angular ones, compared to 40 vol.%), a rapid injectability drop was measured.

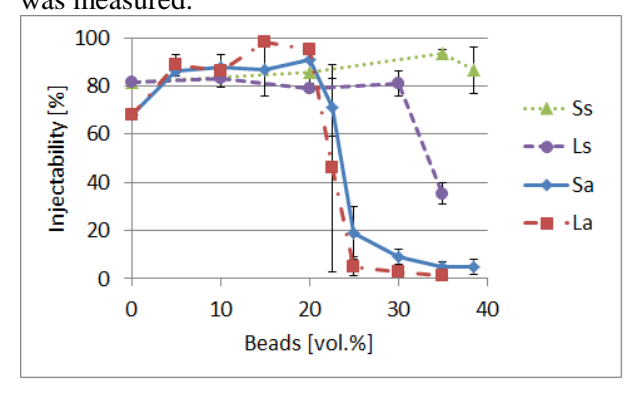


Fig. 1: Injectability results as a function of the bead content. The results with SS and LS were presented in [1].

Table 1. Measured beads size, sphericity and bulk density

Glass beads	d _{50_} ins [μm]	d _{50_} circ [μm]	Spheri- city	Bulk. D. [g.cm ⁻³]
SS	87	87	0.93	1.43
	± 55	± 55	± 0.06	± 0.00
LS	282	282	0.95	1.47
	± 88	± 88	± 0.09	± 0.00
SA	128	232	0.55	1.08
	± 31	± 67	± 0.11	± 0.00
LA	285	482	0.58	1.17
	± 45	± 72	± 0.08	± 0.00

DISCUSSION & CONCLUSIONS: Changing the shape of granules strongly reduced the injectability of pastes made of β -TCP powder, water and glass beads. Similar injectabilities were obtained for the two pastes composed of angular beads (SA and LA).

REFERENCES: ¹ S. Tadier et al. (2014) Acta Biomateriala, DOI: 10.1016/j.actabio.2013.12.018.

